land

Article

Multi-Scenario Land Use Simulation and Land Use Conflict Assessment Based on the CLUMondo Model: A Case Study of Liyang, China

Xiangnan Fan [1], Yuning Cheng [1,*] and Yicheng Li [2]

[1] School of Architecture, Southeast University, Nanjing 210096, China
[2] School of Horticulture and Landscape Architecture, Southwest University, Chongqing 400715, China; leeyeecheng@swu.edu.cn
* Correspondence: 101004222@seu.edu.cn

Abstract: By predicting and analyzing regional land use conflicts (LUCs), the contradictory relationship between urban development and land resources can be revealed, which can assist in achieving the rational use of land resources. Taking Liyang as a case study, this paper simulated land use in 2030 under three scenarios, namely, the natural growth scenario (NGS), economic development scenario (EDS), and ecological protection scenario (EPS), using the CLUMondo model. The ecological risk assessment model was used to measure the LUCs under each scenario. Through the comprehensive analysis of land use conversion, spatial distribution, and the change characteristics of LUCs, optimization strategies for future land use are proposed. The results indicate that (1) the intensity of land conversion under the three scenarios is ranked as EDS > NGS > EPS; (2) there is little change in the LUCs under the EPS, while significant deterioration is observed under the NGS and EDS; (3) the intensity of LUCs is positively correlated with the degree of land use conversion; and (4) in the future, particular attention should be paid to areas around the city center, the Caoshan Development Zone in the northwest, and Nanshan Bamboo Sea in the south, where high-intensity land use conflicts may occur.

Keywords: land use simulation; CLUMondo model; land use/cover change (LUCC); land use conflicts (LUCs)

check for updates

Citation: Fan, X.; Cheng, Y.; Li, Y. Multi-Scenario Land Use Simulation and Land Use Conflict Assessment Based on the CLUMondo Model: A Case Study of Liyang, China. *Land* **2023**, *12*, 917. https://doi.org/10.3390/land12040917

Academic Editors: Eduardo Gomes, Eduarda Marques da Costa and Patrícia Abrantes

Received: 21 March 2023
Revised: 13 April 2023
Accepted: 18 April 2023
Published: 19 April 2023

1. Introduction

As a non-renewable resource necessary for human survival, land is the most basic material for human production and life. It serves as the foundation for the development of a country and society as a whole. As the world's population grows rapidly and urbanization accelerates, limited land resources are supporting larger and more intensive human activities [1]. Inappropriate development and land use have caused a number of significant global problems, such as vegetation destruction, land degradation, and biodiversity loss [2]. Therefore, effectively resolving the conflict between urban development and land resources in order to achieve sustainable land use and maintain regional ecological stability has become an important issue in today's world [2,3]. Land use/cover change (LUCC) refers to changes in the land surface caused by human activities [3]. It reflects the interaction between human activities and natural factors in the regional ecological environment [1], and it is an important factor influencing ecological processes on the Earth, such as biochemical cycling, energy exchange, and soil erosion and deposition [4,5]. In 1992, the United Nations issued "Agenda 21", in which LUCC research was clearly identified as a priority for the 21st century [6]. In 1995, the International Geosphere-Biosphere Programme (IGBP) and the International Human Dimensions Programme (IHDP) on Global Environmental Change jointly proposed the "Land Use/Cover Change Science Research Program", making LUCC-related issues a research priority in countries around the world [7]. In 2005, the

Global Land Project (GLP) was launched jointly by IGBP and IHDP to better continue the LUCC program that started a decade earlier [8]. This project emphasizes the integration of LUCC research, which requires a comprehensive consideration of the coupling relationship between human and natural factors, with research on the interaction between social and ecological systems and on the connections across regions and urban-rural areas. In 2016, the Global Land Project was changed to the Global Land Programme, which continues as a research initiative aimed at understanding, measuring, and modeling the changes in the coupled human-environment system [9]. After almost 30 years of development, research on LUCC has made great progress in theory, methodology, and practice. The main research directions include LUCC monitoring, driving mechanisms, environmental impacts, and simulation. These fields are interrelated and complementary and together form the basic framework of land use and land cover change research [2,10,11].

To respond in a timely manner to the environmental pressures brought by urban development and human demands for land, land use simulation can predict future land change trajectories and development patterns, as well as identify the most appropriate spatial patterns of land use under different future development scenarios. This can provide guidance to urban planning and land policy making [12,13]. At present, the main land use change models are the Markov model, SLEUTH model, system dynamics (SD) model, agent-based model (ABM), cellular automata (CA) model, CLUE-S model, etc. [14]. Each of these models has its own unique characteristics and scales of applicability. The Markov model can quantify the conversion state and conversion rate of land use types, but it cannot describe spatial changes. The SLEUTH model is suitable for urban growth simulation and long-term forecasting, but it takes less account of social and economic factors. The SD model can reflect the interrelationships among the structure, function, and dynamic behavior of complex systems, but it is difficult to handle spatial information and lacks the ability to describe the spatial pattern of land use. The agent-based model (ABM) is limited in its applicability to certain regions and scenarios and has difficulty representing the spatial behavior of a subject [15,16]. The CA model is better at representing the neighborhood effects, but its conversion rules are based on empirical statistics or expert knowledge, making it susceptible to human factors. The CLUE-S model can simulate the changes in multiple types of land use and reflect the situation of land use change in terms of time, space, and quantity. It is particularly suitable for studying land use/cover change in small-scale regions. The CLUMondo model is the latest improved version of the CLUE-S model. It has inherited all the advantages of the CLUE-S model and addresses the shortcomings of its inadequate consideration of macro and non-spatial factors [17]. The CLUMondo model can convert macro factors, such as policies into land use demand parameters, comprehensively considering direct and indirect demand for different types of land area. It can also spatially allocate different intensities of land service demand based on land suitability and select the allocation order according to the strength of competition. The study case in this paper is Liyang, a county-level city in China, which is a small-scale region currently facing the challenge of balancing the conflicting objectives of economic, environmental, and social benefits while undergoing rapid urbanization. Therefore, the CLUMondo model was selected for the city to perform multi-scenario land use prediction in order to explore the possibilities of future land use changes and spatial patterns in the study area.

During the process of land use, disagreements among stakeholders over the use, allocation, quantity, and distribution methods of the land can result in land use conflicts (LUCs) [1]. They reflect the discordance and imbalance between the allocation of land use and the needs of social development in human-environment relationships, such as conflicts between urban expansion and the protection of basic farmland or ecological conservation. Severe LUCs can pose a threat to ecological and food security, thereby limiting regional sustainable development [18]. They can also lead to disputes over land rights and interpersonal conflicts, and they can even become important factors affecting social stability [19]. Scholars have analyzed LUCs from the perspectives of economics, geography, ecology, and sociology. Qualitative analysis methods commonly used include participatory survey methods, logical framework approaches, and game theory analysis. While these methods assist researchers in understanding the mechanisms behind and finding solutions to land use conflicts, quantitatively measuring such conflicts remains a challenge [20]. Commonly used quantitative analysis methods include suitability assessment [21,22], multicriteria analysis [23–25], ecological risk assessment [1,20], and the pressure-state-response (PSR) model [18,26–28]. Based on the theory and methods of landscape ecological risk assessment, ecological risk assessment is a model for measuring conflicts. It constructs a conflict index by considering risk sources, risk receptors, and risk effects. The model creates a "comprehensive spatial conflict index = spatial complexity index + vulnerability index − stability index" equation to quantify spatial conflicts. This method can accurately identify conflict locations and spatial characteristics, as well as reveal regional ecological risks caused by inappropriate spatial structures of land use. Due to various ecological problems in Chinese cities caused by rapid urbanization, and the fact that this method can objectively and effectively characterize the pressure of human interference and natural degradation, this study selected the ecological risk assessment model to measure land use conflicts in the study region.

Currently, research on land use simulation is mostly focused on revealing the characteristics of land use conversion [29,30], exploring future development scenarios [31–33], and evaluating future ecosystem services [16,34,35]. The research on land use conflict is mainly focused on identifying the spatiotemporal evolution characteristics [36–38] and driving factors of current land use conflicts [39,40]. Few studies have explored the possible development trends of LUCs by land use simulation and prediction. This limits the comprehensive and profound analysis of land use conflict issues and also has a restrictive effect on the formulation of future land use management policies. Especially for China, where development is rapid and land resources are extremely scarce, spatial planning strategies that are forward-looking and can predict land use issues are particularly important. Since 2019, territorial spatial planning has become an important development strategy in China. Its main purpose is to coordinate land use and development intensity among different regions based on their resource endowments and comparative advantages, so as to avoid the escalation of regional land use conflicts and contradictions caused by the different positioning of planning functions [41,42]. Therefore, government policies need to consider future land management, and research on land use conflicts (LUCs) should expand to include simulations of potential future changes.

In light of the limited focus on future land use conflicts in academic research, this paper uses the Liyang in Jiangsu Province as a case study to provide empirical evidence for predicting potential future trends in land use conflicts through multi-scenario land use simulations. This paper also suggests strategies for spatial governance and optimizing land use patterns to address and reduce land use conflicts. The research provides a valuable reference for future studies on the sustainable use of regional land resources and territorial spatial planning. The study's specific research objectives include (1) studying land use changes in Liyang in 2030 under different scenarios; (2) examining the spatial characteristics of future land use conflicts (LUCs) in Liyang; and (3) determining strategies and key areas for spatial optimization in Liyang.

2. Materials and Methods

2.1. Study Area

Liyang is a city at the county level in Jiangsu Province, situated between 31°09′–31°41′ north latitude and 119°08′–119°36′ east longitude. It is located at the intersection of three provinces in the Yangtze River Delta region. It has a variety of topographical features, including low mountains, hills, plains, and polders, and has a total area of 1535 km^2. The city is interwoven with rivers and lakes; it has low mountains and hills in the south and northwest and plains and polders in the center (Figure 1). Since the early 1990s, tourism has become an important industry in Liyang, not only solving people's food and clothing problems but also driving rapid economic and urban development. By 2020, Liyang's urbanization rate had risen from less than 10% in the 1980s to 63%, and its total GDP had increased from 28 million in the 1980s to 108.6 billion (Figure 2). In the past 40 years of its development, Liyang's tourism industry has become a breakthrough point for deepening economic reform in the city. In form, the industry has transformed from scenic-spot tourism to all-for-one tourism, emerging as a new model for tourism development. This has led to the rapid development of the city's tertiary industry, which increased from 15% in the 1980s to 45% in 2020. Liyang was selected in the second batch of national all-for-one tourism demonstration zones in 2020. In the future, Liyang will continue to leverage all-for-one tourism as a catalyst for the city's high-quality development. Therefore, eliminating current and potential land use conflicts and forming a coordinated development system of urban development and an ecosystem in the region are key considerations in Liyang's land use planning.

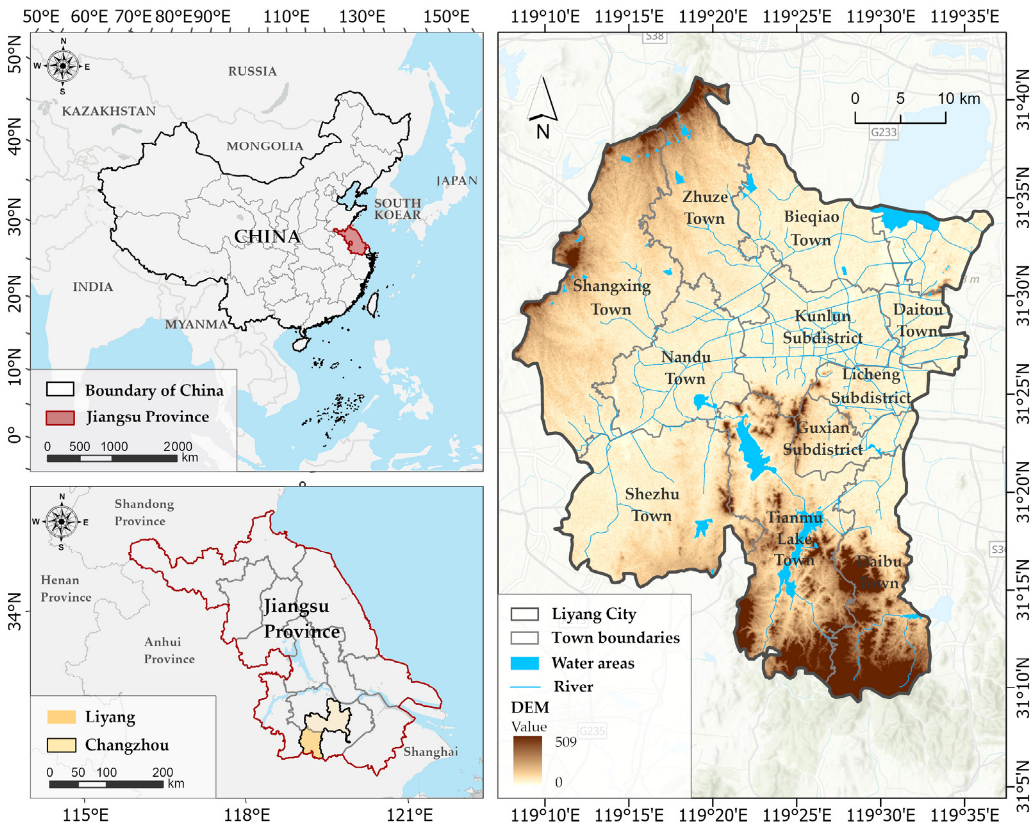

Figure 1. Location and digital elevation map (DEM) of Liyang.

2.2. Data Sources and Processing

The primary data used in this research were resampled to a 90 m precision raster graphic and georeferenced using the Albers Conical Equal Area projection in ArcGIS. These data included land use, topographic, meteorological, soil, position, and socio-economic data, as listed in Table 1. The remote-sensing images were analyzed using ENVI5.3 to identify seven types of land use: cultivated land, woodland, grassland, water area, rural settlements, urban, and other construction land and unused land. Meteorological data were initially obtained from meteorological stations and were converted into grid format by spatial interpolation using ArcGIS 10.6. For land use simulation, all data were converted into ASCII format in CLUMondo, and the ecological sources in the study area were set as restricted areas.

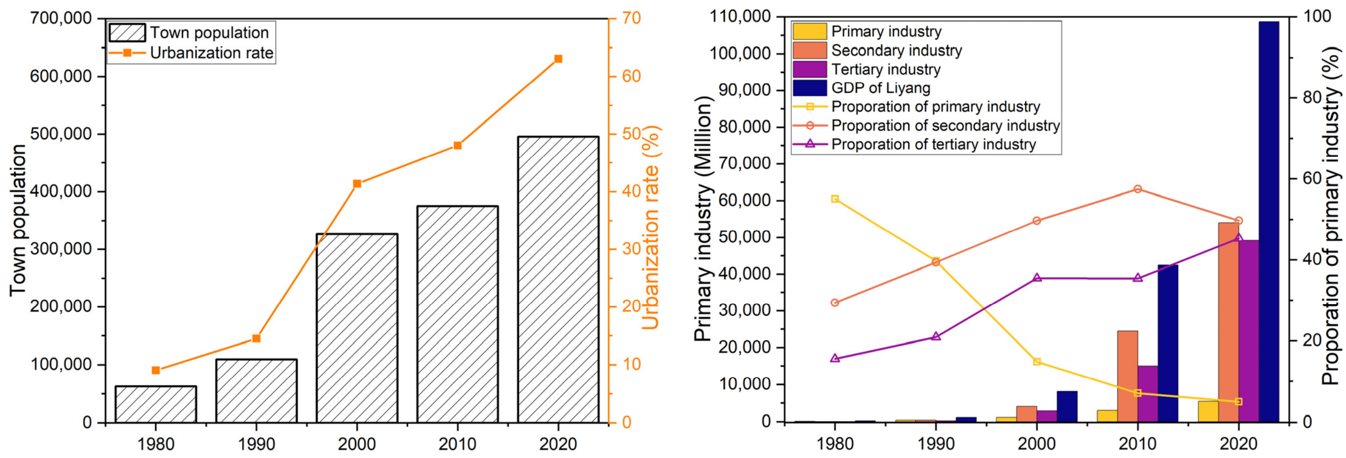

(**a**) (**b**)

Figure 2. Development of Liyang from 1980 to 2020. (**a**) Urbanization process; (**b**) Industry development process.

Table 1. Data sources and description.

Category	Data	Unit	Year	Data Source
Land use	Remote-sensing images	-	2010, 2020	United States Geological Survey (USGS)
	Land use maps	class	2010, 2020	Interpreted from remote-sensing images
Topographic	DEM	m	2010, 2020	Geospatial Data Cloud
	Slope	°	2010, 2020	Extracted from DEM data
	Aspect	-	2010, 2020	
Meteorological	Annual total precipitation	mm	2010, 2020	China Meteorological Data Service Centre
	Annual average temperature	°C	2010, 2020	
Soil	Soil water content	m^3	2010, 2020	National Tibetan Plateau Data Center
	Soil salinity	%	2010, 2020	World Soil Information (ISRIC)
Position	Distance to major rivers	km	2010, 2020	OpenStreetMap
	Distance to main traffic	km	2010, 2020	
	Distance to township centers	km	2010, 2020	
Socio-economic	Population density	people/km^2	2010, 2020	Statistical Yearbook of Liyang City
	Per capita GDP	10^4 yuan	2010, 2020	
	Fixed assets investment	10^8 yuan	2010, 2020	
	Nighttime light	-	2010, 2020	National Tibetan Plateau Data Center

2.3. Methods

Figure 3 illustrates the overall research structure. The study area's land use in 2030 was projected using the CLUMondo model under various scenarios. The ecological risk assessment model was used to evaluate the LUCs in the region from 2010 to 2030. Some spatial analysis approaches, such as standard deviational ellipse and hot spot analysis, were used to quantitatively describe land use features. Based on these analyses, strategies for land management and planning were proposed.

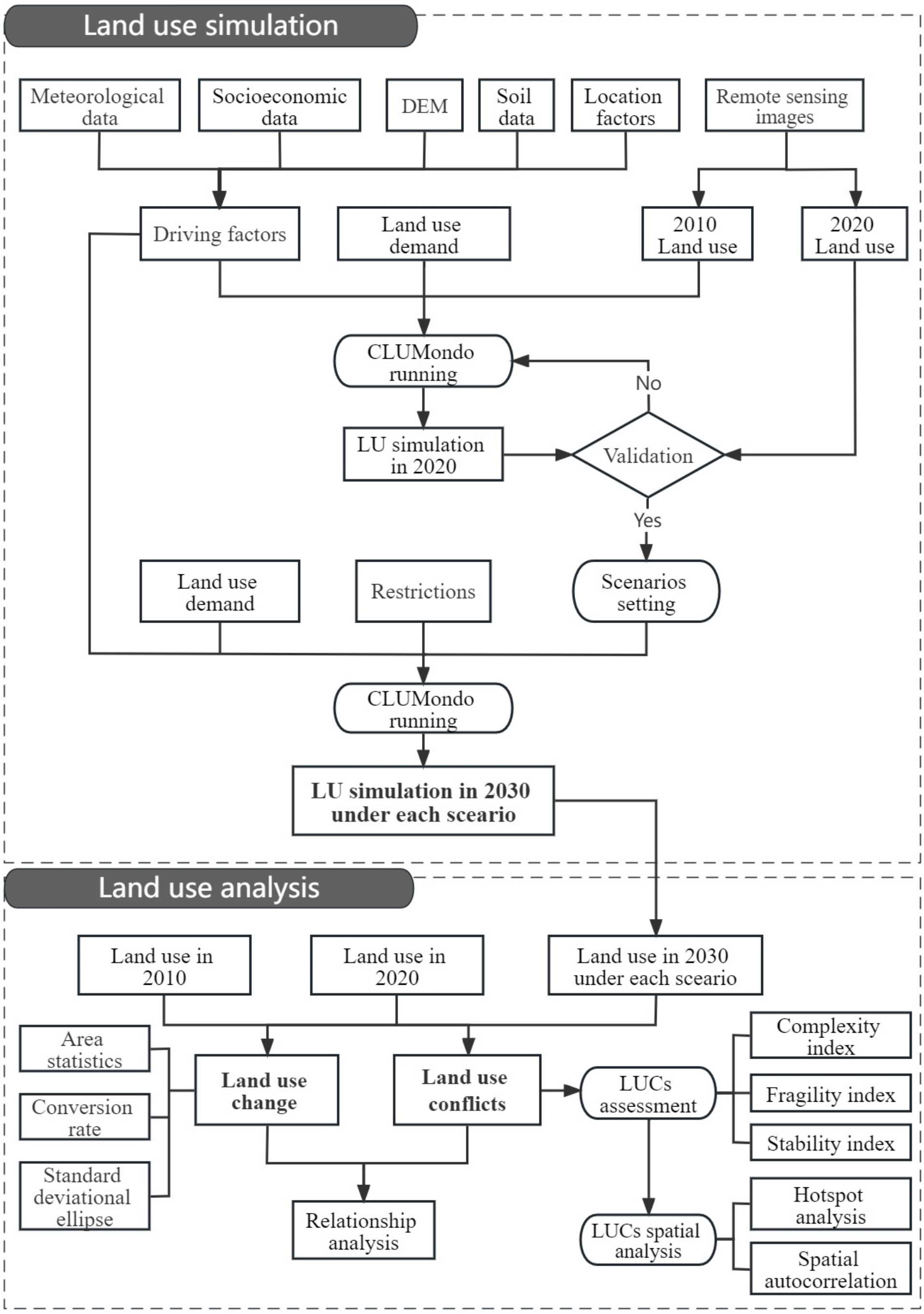

Figure 3. Technical flow chart.

2.3.1. Dynamic Degree of Land Use

The dynamic degree of land use reflects the conversion rate and intensity of land use change in the study area [43]. The single dynamic degree indicates the conversion rate of a certain type of land during the conversion period [44]. The calculation formula is as follows:

$$K_i = \frac{S_b - S_a}{S_a} \times \frac{1}{T} \times 100\% \tag{1}$$

where K is single land use dynamic degree; i is a certain land use type; S_a is the area of a certain land use type before the conversion; S_b is the area after the conversion; and T is the conversion period.

The comprehensive dynamic degree represents the change rate of all land use types and reflects the overall land use stability in the study area [45]. A higher value indicates more active land use changes and poorer overall stability. The formula is as follows:

$$S = \left[\sum_{i=1}^{n}\left(\frac{\Delta S_{i-j}}{S_i}\right)\right] \times \frac{1}{T} \times 100\% \tag{2}$$

where S is the comprehensive land use dynamic degree; S_i is the total area of land use type i; ΔS_{i-j} is the total area of land use type i converted in and out; and T is the transfer period.

2.3.2. Land Use Conflict Assessment Model

When a land ecosystem experiences a significant disruption, its spatial pattern alters, leading to disruptions in natural processes, reduced biodiversity, and harm to the region's ecological security [46]. This occurrence demonstrates the clash between the spatial arrangement of land use and the natural environment. Typically, the lower the ecological risk posed by a land use structure, the less severe the land use spatial conflict [18]. As a result, the land use conflict assessment model was developed by drawing on the "risk source-risk receptor-risk effect" ecological risk evaluation model. The formula is as follows:

$$LUCI = CI + FI - SI \tag{3}$$

where $LUCI$ is the index of land use conflict; CI is the complexity index; FI is the fragility index; and SI is the stability index. As a reliable measure of risk sources, landscape complexity reflects external pressures from human activities and intensive land use. The area-weighted mean patch fractal dimension (AWMPFD) [20] is employed to describe the intricacy of land use patches and indicate the extent to which neighboring landscapes affect current landscape units. A higher value signifies a more complex landscape patch boundary and a greater likelihood of disturbance from human activities [20,47]. The calculation formula is as follows:

$$CI = AWMPFD = \sum_{i=1}^{m}\sum_{j=1}^{n}\left[\frac{2\ln(0.25P_{ij})}{\ln(a_{ij})} \times \left(\frac{a_{ij}}{A}\right)\right] \tag{4}$$

where P_{ij} is the perimeter of the j-th patch of the i-th land-use type; a_{ij} is the patch area of the j-th patch of the i-th land use type; A is the total landscape area; m is the number of patches; and n is the number of land use types. The index values have been linearly adjusted to fall within the [0, 1] range in order to simplify subsequent calculations. The fragility index measures the responsiveness of spatial patches to external pressures and indicates the risk receptors' carrying capacity [47]. The lower the resilience of receptors, the more vulnerable the spatial patch is to external disturbance and the higher the level of land use conflict [48]. According to the previous studies [48–51] and the characteristics of regional urbanization, the fragility values of seven land use types in the study region were determined to be: urban and other constructed land (7), rural settlements (6), unused (5), grassland (4), water (3), farmland (2), and woodland (1). The calculation formula is as follows:

$$FI = \sum_{i=1}^{m}\sum_{j=1}^{n} F_{ij} \times \frac{a_{ij}}{A} \tag{5}$$

where F_{is} is the fragility degree of the j-the patch of land-use type i; a_{ij} represents the area of the j-th patch of land use type i; A represents the total area of the landscape; m is the number of patches; and n stands for the number of land use types. To make calculations easier, the results were linearly adjusted to fall within the [0, 1] range. As a key measure of the risk effect, landscape stability is assessed using the patch density index (PD), which indicates the degree of landscape fragmentation. A higher value signifies a more fragmented landscape, poorer land stability, and more severe land use conflict [1,20]. The calculation formulas are as follows:

$$SI = 1 - \frac{PD - PD_{min}}{PD_{max} - PD_{min}} \quad (6)$$

$$PD = \frac{n_i}{A} \quad (7)$$

where PD is the index of patch density; PD_{min} and PD_{max} represent the minimum and maximum values of PD; n_i is the number of landscape patches of land use type i; and A is the total area of the landscape.

2.3.3. Simulation of Future Land Use

As the latest iteration in the series of Conversion of Land Use and its Effect (CLUE), CLUMondo is a dynamic and spatially explicit land use model capable of simulating changes in both land cover and land use intensity [52]. Its land use simulation is based on a combination of an empirical analysis of location suitability and a dynamic assessment of the interactions between land use systems [53]. The demand for goods and services, spatial restrictions, and competition between different land use types are comprehensively considered in the CLUMondo model, effectively improving on previous land use simulation methods that focused only on the quantity of land conversion [54,55].

1. Scenario settings

Three simulation scenarios were established to examine the future development trend of land systems in the study region under different conditions, based on government planning, economic development objectives, and environmental protection demands [56–58].

The natural growth scenario (NGS) refers to a situation where the study area would not experience sudden natural disasters, such as droughts and floods, in the next decade or so, and was not strongly interfered with by external factors. The future transformation followed the trend of land use change in the past (2010 to 2020). According to the government's plan, the urbanization rate will reach 80% by 2030 (17% higher than in 2002), and the city's GDP will need to increase by about 250 billion yuan (about 140 billion yuan higher than in 2020) (Table S1).

The economic development scenario (EDS) focused on economic benefits by expanding the area of built-up land, especially the urban area, traffic land, and industry land. As a result, under this scenario, the growth rate of rural areas was set to be roughly equivalent to that under the NGS, while the growth rate of urban and other construction land was increased by 30% compared to the NGS.

The ecological protection scenario (EPS) aimed to enhance the ecological environment and the services it provides. It took into account the need for strict ecological boundaries and restoration efforts in government planning. This scenario assumed that the area of ecological land in the study area would increase by 10% by 2030. In addition, important ecological sources in this study area include the planned ecological red line area, so these large ecological patches were set aside as conservation areas that could not be converted.

The simulation of different scenarios was realized by different parameter settings, including by adding constraint conditions and defining the conversion matrix and conversion resistance coefficient.

2. Parameter setting for CLUMondo model

Based on previous studies [1,14,32,34,43,59–63] and data availability, 14 independent variables were selected to explain the location suitability of land use (Table S2). A total of 2 factors with high correlation values (above 0.8) were eliminated, and a total of 12 driving factors of LUCC were determined, as shown in Figure S1. Logistic regression analyses were carried out for each land use type and driving factor to obtain "AUC" values, which represent the accuracy of the calculated regression (Table S3).

Six land use service demands (crop production, woodland area, grassland area, water area, rural settlements area, and urban and other construction land area) were calculated independently under different scenarios (Table S4). The annual changes in each service were determined by linear interpolation between the corresponding data in 2010 and 2020. The NGS projected the future land system using the same trend as before. The grey theory is known for its unique ability to make accurate predictions using limited data and uncertain factors [64]. The GM (1.1) model is often used as a forecasting tool within the grey theory and was used in this scenario to calculate the demand for land use services. In EDS, the change rate of rural settlements was set according to the previous decade. The change rate of urban and other construction land was set 30% higher than before, as the construction of characteristic towns, tourism facilities, and transport networks will be greatly developed for all-for-one tourism in the future. In EPS, the areas of woodland, grassland, and water in 2030 were set to increase by 10%. Ecological sources are large patches that provide important ecosystem services, and these should be well-conserved. Identified in a previous study [65], they were determined to be spatial restrictions for the land use simulation under the EPS (Figure S2).

Conversion resistance is a measure of how easily land can be converted. It ranges from 0, which means easy conversion, to 1, which means the change is irreversible. This reflects the convertibility of the land. Each land use type was assigned a specific resistance value under different simulation scenarios, as shown in Table S5. The conversion matrix shows the potential for different types of land use to be converted into one another. The values in the matrix are defined as '1' for allowed conversion, and '0' for not allowed conversion. In this study, the simulations under the NGS and EDS had the same conversion matrix, with the matrix having different values of ecological land than those of the matrix under the EPS, as shown in Table S6.

3. Model validation

The accuracy of the CLUMondo model was checked by comparing its 2020 simulation with the actual land use map from 2020. First, based on the 2010 land use map and the natural growth scenario parameter setting, the 2020 land use simulation was carried out. Then, the Map Comparison Kit (MCK) was used to perform a cell-by-cell comparison using the Kappa algorithm. Kappa statistics, including Kappa, Kappa Histo (KHisto), and Kappa Location (KLoc), were calculated for the whole map and each land use type. Generally, a Kappa value greater than 0.75 indicates good agreement between the two maps and high reliability of the land use simulation. A Kappa value between 0.4 and 0.75 indicates fair agreement, while a value less than 0.4 indicates poor agreement [66,67].

2.3.4. Spatial Autocorrelation Analysis

Spatial autocorrelation analysis was used to determine the heterogeneity of the spatial distribution of LUCs, including the global spatial autocorrelation index Moran's I and the local spatial autocorrelation index LISA [68–70]. Moran's I indicates the extent to which similar values of a variable are clustered together in space. The value range of Moran's I is −1–1. If a Moran's I value is greater than 0, the spatial correlation is positive, meaning that the locations with similar attributes of the variable are clustered together. When Moran's I is less than 0, it indicates that there is a negative spatial correlation, meaning that locations with similar values for a variable are spread out or dispersed in space. If Moran's I is equal to 0, it means that there is no spatial correlation. LISA measures the degree of spatial clustering of a specific location surrounded by similar or dissimilar values. The result is shown in a map of high and low clustering, which is useful for identifying the spatial pattern of local autocorrelation. The calculation formulas are as follows:

$$Moran's\ I = \frac{n}{\sum_{i=1}^{n}\sum_{j=1}^{n} W_{ij}} \times \frac{\sum_{i=1}^{n}\sum_{j=1}^{n} W_{ij}(x_i - \overline{x})}{\sum_{i=1}^{n}(x_i - \overline{x})^2} \tag{8}$$

$$LISA = \frac{n(x_i - \overline{x})}{\sum_i (x_i - \overline{x})^2} \sum_i W_{ij}(x_i - \overline{x}) \tag{9}$$

where n is the total number of conflict cells; x_i and x_j represent the values of a variable x at two different spatial locations i and j; $\overline{x}$ represents the average value of the variable; and W_{ij} is the spatial adjacency matrix.

3. Results

3.1. Validation of CLUMondo Model

The land use status in 2020 and the land use simulation of the study region in 2020 are shown in Figure 4. The Kappa coefficients are shown in Table S7. With the exception of the unused land, the Kappa coefficient of each land use type was greater than 0.6. This is because the unused land represented only 2.2 percent of the area and was scattered and susceptible to human behavior, resulting in high simulation difficulty and low simulation accuracy. In general, the overall Kappa coefficient was greater than 0.75, and it can therefore be considered that the CLUMondo model was reliable for simulating future land use changes in the study area.

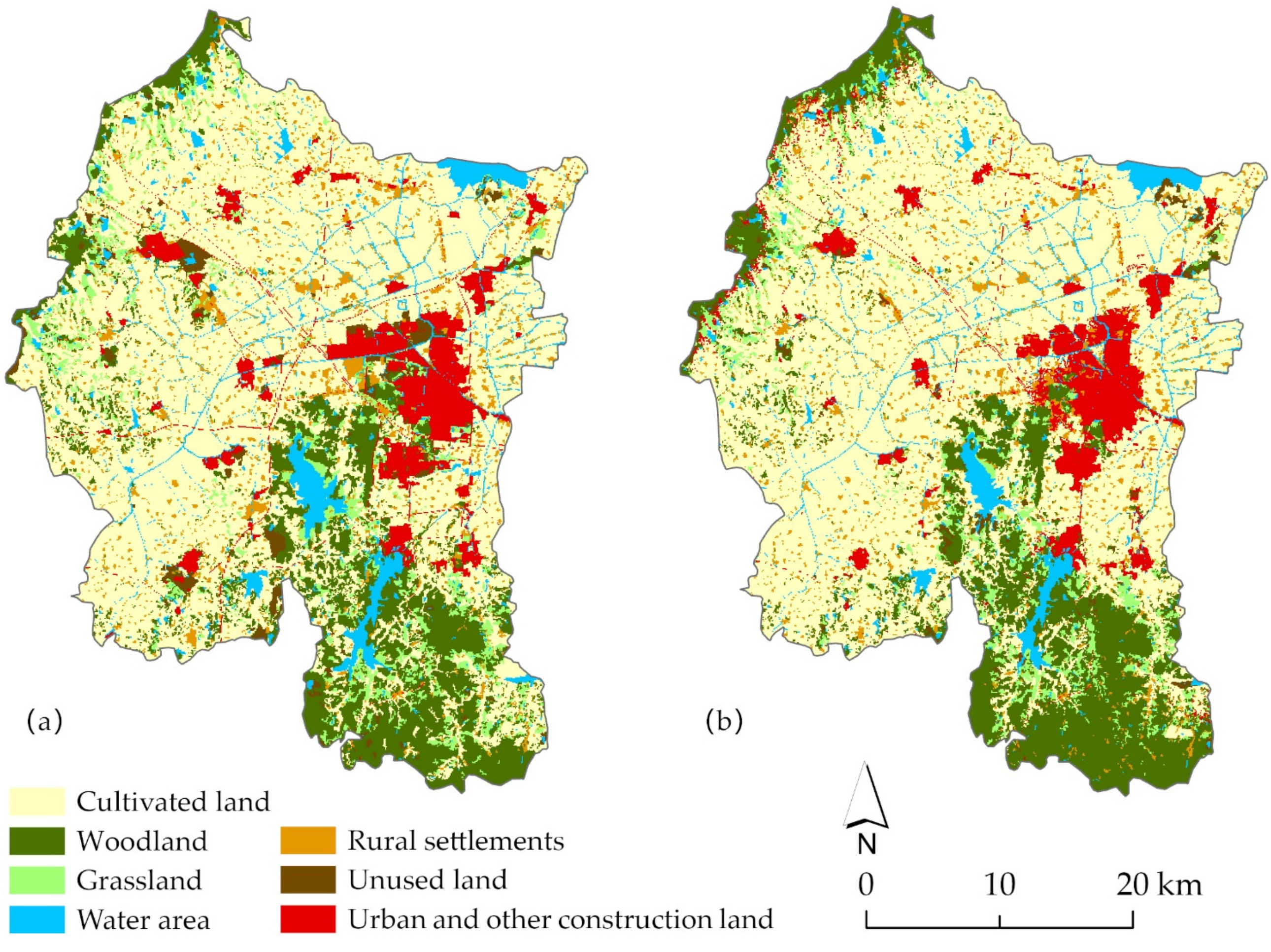

Figure 4. (**a**) 2020 land use map; (**b**) land use simulation of 2020.

3.2. Simulation Results of Future Land Use

The spatial distributions of the land use simulation for 2030 are shown in Figure 5. The land use areas and change rate are shown in Figure 6. The area conversion graphs of each land use type under the defined scenarios are shown in Figure 7. Generally, the water area and rural settlements changed slightly under the three scenarios. Significant changes occurred in the cultivated land, grassland, unused land, and urban and other construction land. In all scenarios, there was a large decrease in cultivated and unused land, while urban and other construction land increased significantly.

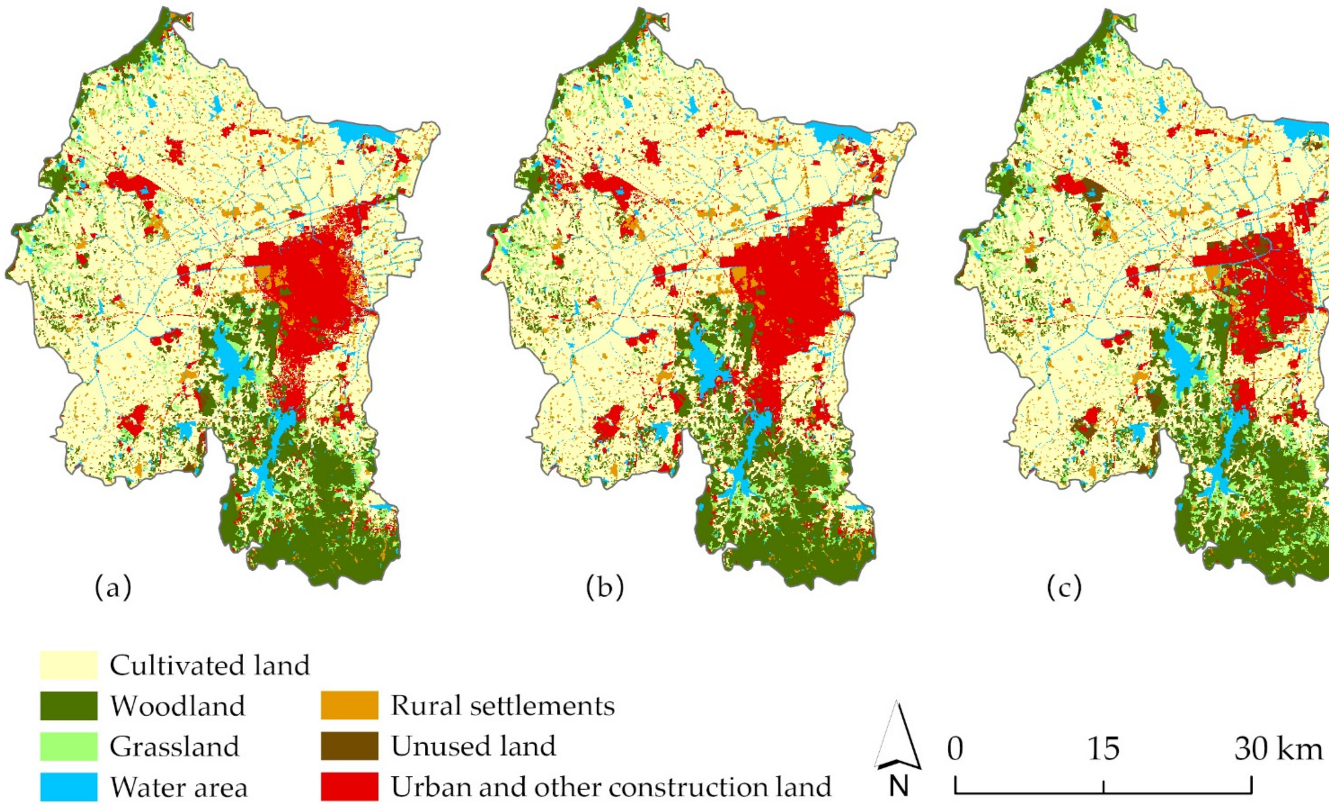

Figure 5. Results of land use simulation in 2030 under different scenarios. (**a**) NGS; (**b**) EDS; (**c**) EPS.

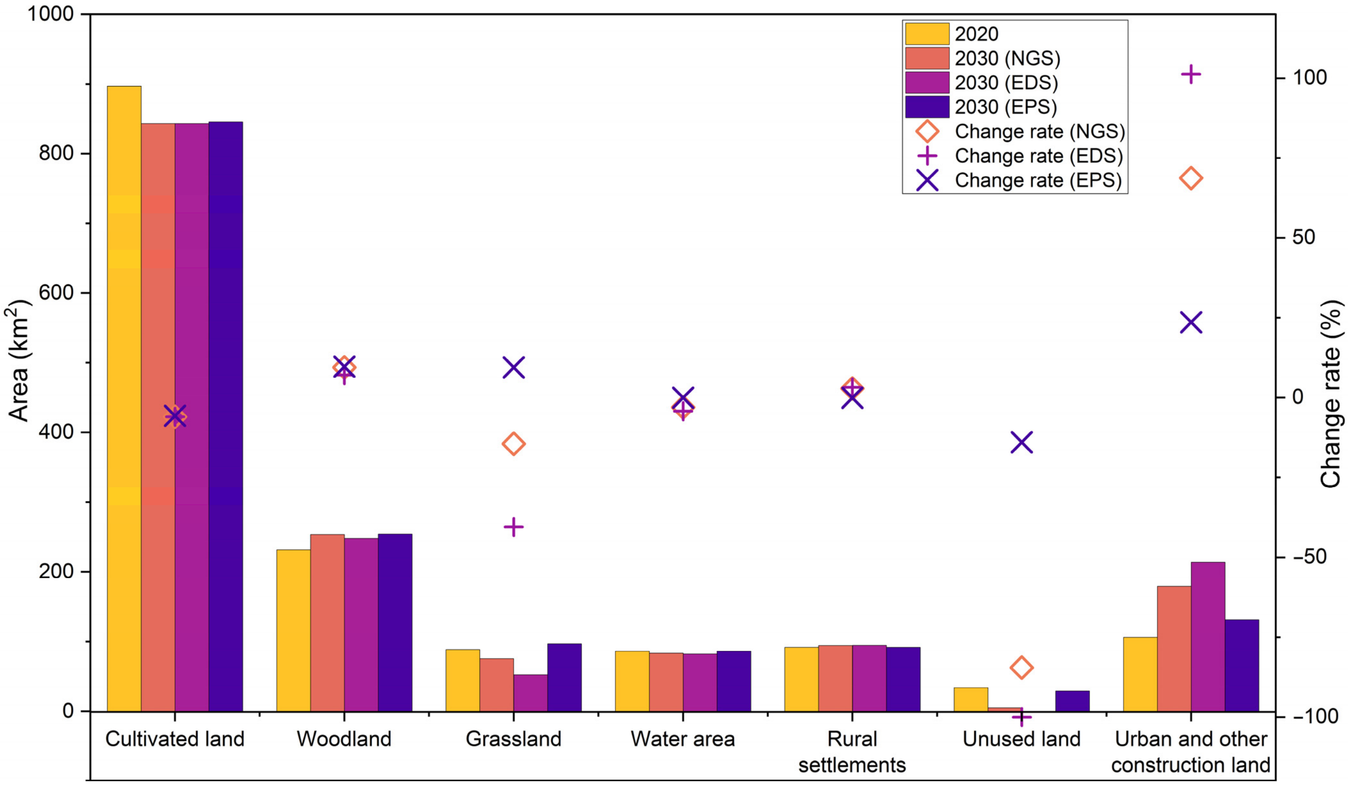

Figure 6. Land use changes under different scenarios for 2030.

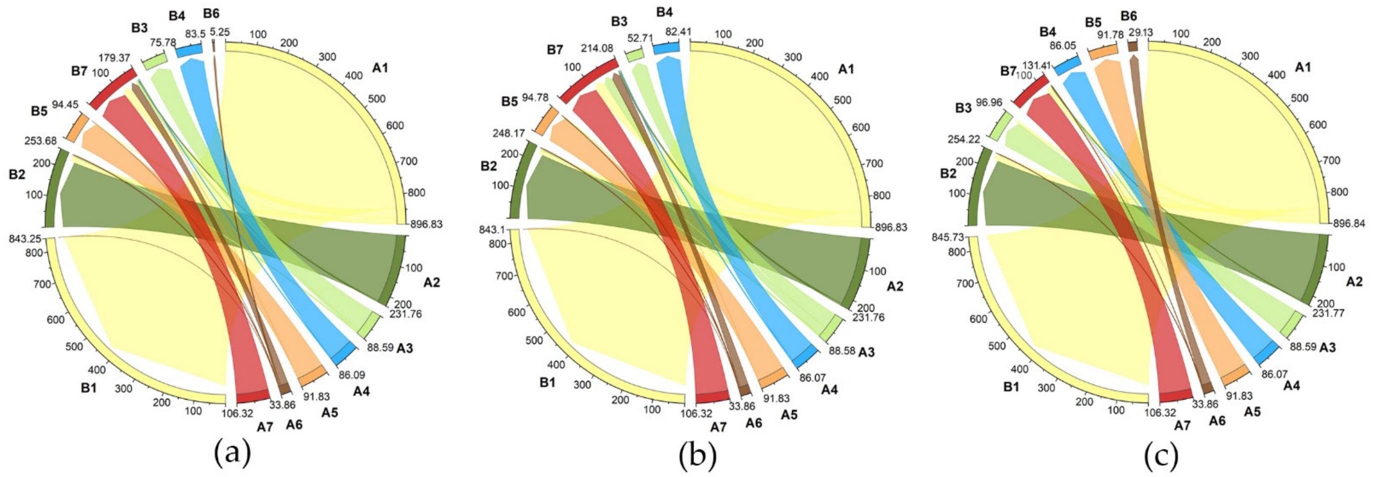

Figure 7. Land use conversion area chord diagrams. (**a**) NGS; (**b**) EDS; and (**c**) EPS. A1–A7 are the land use types in 2020; B1–B7 are the land use types in 2030; 1–7 represent cultivated land, woodland, grassland, waters, rural settlements, unused land, and urban and other construction land.

Under the NGS, the urban and other construction land expanded mainly around the original urban center, recording an area of 73 km^2 and a growth rate of 68.69%. These conversions were mainly derived from the cultivated land and unused land, which accounted for 44.13% and 34.66%, respectively. A total of 53.74 km^2 of the cultivated land was converted into urban and other construction land (59.98%), woodland (34.34%), and rural settlements (5.68%). A total of 28.61 km^2 of the unused land was converted, of which 88.51% was converted to urban and other construction land, 10.9% to woodland, and 0.59% to cultivated land and rural settlements. The woodland increased by 9.46% and the grassland decreased by 14.46%, while the change rates of the rural settlements and water area were no more than 5%. Premised on the economic development of the EDS, the expansion of built-up land around the urban center rapidly led to the formation of one large area, with a newly added area of 107.77 km^2 and a high growth rate of 101.33%. The conversions were derived from every land use type, of which the cultivated land, grassland, and unused land accounted for more than 90%. A total of 53.96 km^2 of the cultivated land was converted to the urban and other construction land (71.71%), woodland (27.8%), and rural settlements (0.5%). Nearly 87% of the converted grassland became built-up land, amounting to an area of 31.23 km^2, while the remaining 13% became woodland. All of the unused land with an area of 33.86 km^2 was converted, 84.5% of which to the urban and other construction land, 9.23% to woodland, 5.57% to rural settlements, and 0.7% to cultivated land. The woodland and rural settlements increased by 7.08% and 3.2%, respectively, while the water area decreased by 4.25%. The scale of built-up land expansion under the EPS was significantly smaller than that of those under the other two scenarios. It was because the amount and distribution of built-up land were well-controlled for the sake of ecological protection. Further, the urban and other construction land increased by only 25.1 km^2, with a change rate of 23.58%. The conversions mainly derived from the cultivated land (78.33%), woodland (12.96%), and unused land (8.46%). Both the woodland and grassland increased by around 10%, while the unused land decreased by around 14% and the cultivated land decreased by around 6%. The water area and rural settlements remained almost unchanged.

3.3. Characteristics of Land Use Conflicts

The spatial distributions of the LUCs and the proportion of the area occupied by each conflict level are shown in Figure 8 and Table 2. The average conflict index increased in 2030 compared to 2020 in all scenarios, with the highest increase observed under the EDS. In 2020, high-level conflict areas accounted for 34.3%, were mainly scattered along rivers and traffic arteries, and were locally mixed with higher-level conflict areas, which accounted for 2.16%. The LUCs in 2030 under the EPS remained basically unchanged, while there were significant changes under the NGS and EDS. The area of high-level LUCs under the NGS increased slightly by 0.39%. The area of higher-level LUCs increased by about 1%, forming a ring-shaped pattern around the city center. Under the EDS, the area of high-level and higher-level LUCs increased by 1.33% and 4.7%, respectively. In terms of the spatial distribution of the LUCs, the area of the city center changed the most. Its inner area increased from a low to a moderate level, and its outer ring-shaped higher-level area was more significant than it was under the NGS. In addition, the originally scattered higher-level areas became more aggregated, and new agglomeration centers developed on the northwestern and southern sides of the study area.

Table 2. Statistics for LUCs index measurement.

Conflict Level	Conflict Index Range	Area Ratio (%)			
		2020	2030		
			NGS	EDS	EPS
Lower	0–0.2	10.61	11.00	11.82	10.30
Low	0.2–0.4	19.59	16.90	16.30	19.19
Moderate	0.4–0.6	33.33	34.27	29.39	33.22
High	0.6–0.8	34.30	34.69	35.63	34.78
Higher	0.8–1	2.16	3.15	6.86	2.52
Average conflict index		0.492	0.500	0.508	0.498

Figure 9 illustrates the area of each land use type in the different levels of land use conflict. In 2020 and 2030, more than 90% of both the woodland and water area occupied the low and lower LUC levels, indicating that these two land use types were in a stable state. Apart from its absence under the EDS, the unused land remained in the low and lower LUC levels in both 2020 and 2030. Over 90% of the grassland occupied the low and moderate LUC levels, except for under the EDS, where it was around 80%. The areas of these two types of land were small in size within the study area, so even if their changes were significant, they did not have a great impact on the LUCs. More than 90% of the cultivated land was distributed in the moderate and above LUC levels, with more than 50% being distributed in the high and higher levels, indicating that the cultivated land was highly variable. The distribution of built-up land varied greatly across the different LUC levels. In 2020, 74% of the rural settlements occupied the moderate LUC level. By 2030, more than 50% were in the high and higher LUC levels in all scenarios, with more than 90% occupying these levels under the EDS. The urban and other construction land accounted for only about 6% of the high and higher LUC levels in 2020, while it increased in 2030 to 42% under the NGS, 58.85% under the EDS, and 19.42% under the EPS.

The global spatial autocorrelation test was performed for the LUCs in 2020 and 2030, as shown in Table 3. The p-values were all less than 0.01, and the z-scores were all greater than 2.58, indicating that the results of the spatial autocorrelation confidence test were reliable, i.e., the conflict levels of the different spatial units were not randomly distributed. The value of Moran's I was 0.76 in 2020 and increased to more than 0.8 in 2030, indicating that the clustering of LUCs will increase in the future and that the EDS recorded the strongest clustering effect among the three scenarios. The calculation results of the local index of spatial autocorrelation (LISA) for the LUCs are shown in Figure 10. In 2020, hot spots were scattered in the study area, mainly along rivers and traffic arteries. In 2030, there were no major changes under the EPS. Under the NGS and EDS, there was an obvious belt-shaped hot spot aggregation area around the city center, and the original hot spot areas had all expanded. Compared to the EPS, there were also significant hotspot clustering areas on the northwest and south sides of the city under the EDS. The cold spots were clusters of low-level conflict, and these were mainly concentrated in large areas of water and woodland; the overall change from 2020 to 2030 was not significant. However, the cold spot areas within the city center had greatly reduced by 2030 and had almost disappeared under the NGS and EDS.

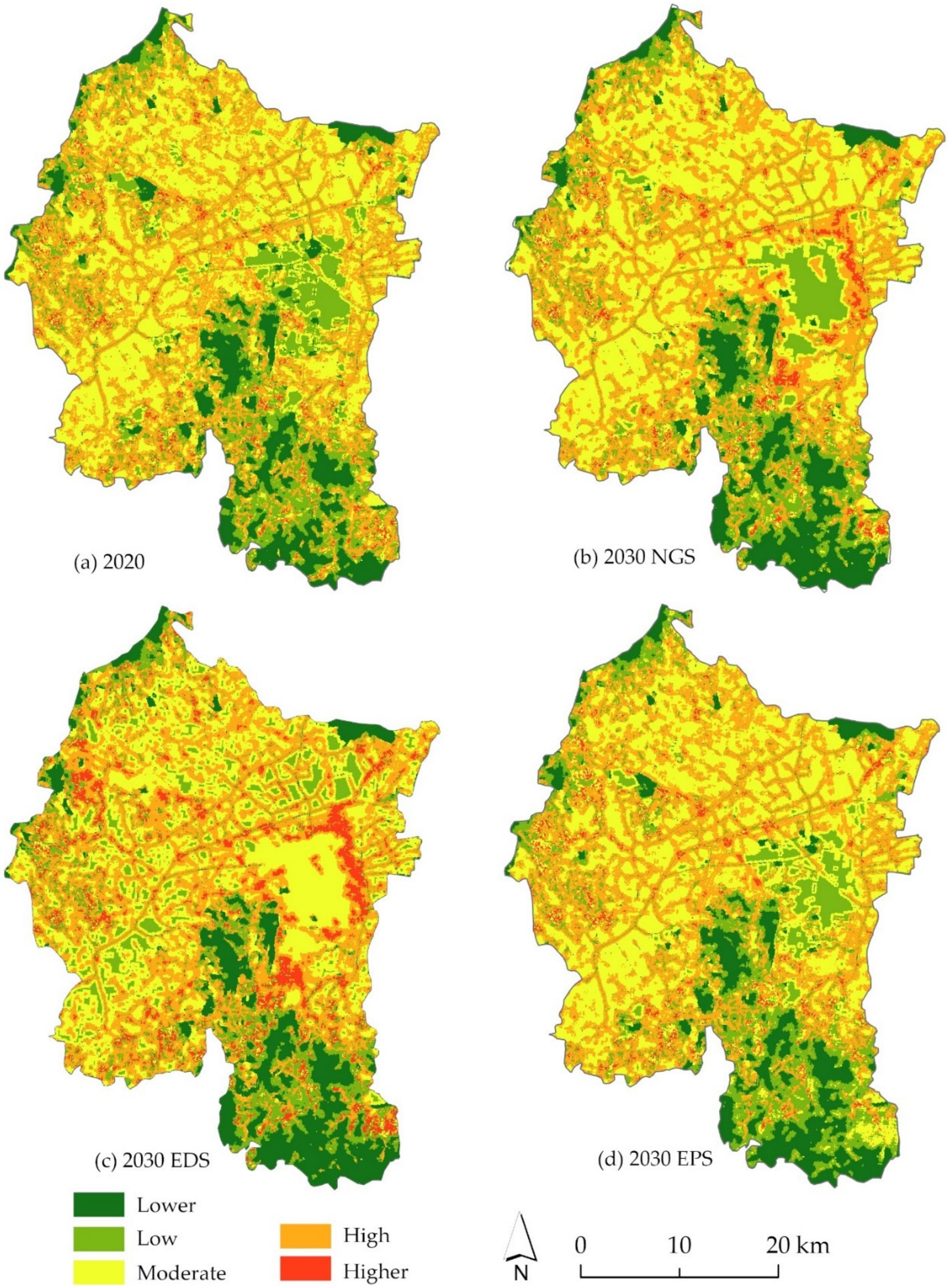

Figure 8. Spatial distribution of land use conflicts.

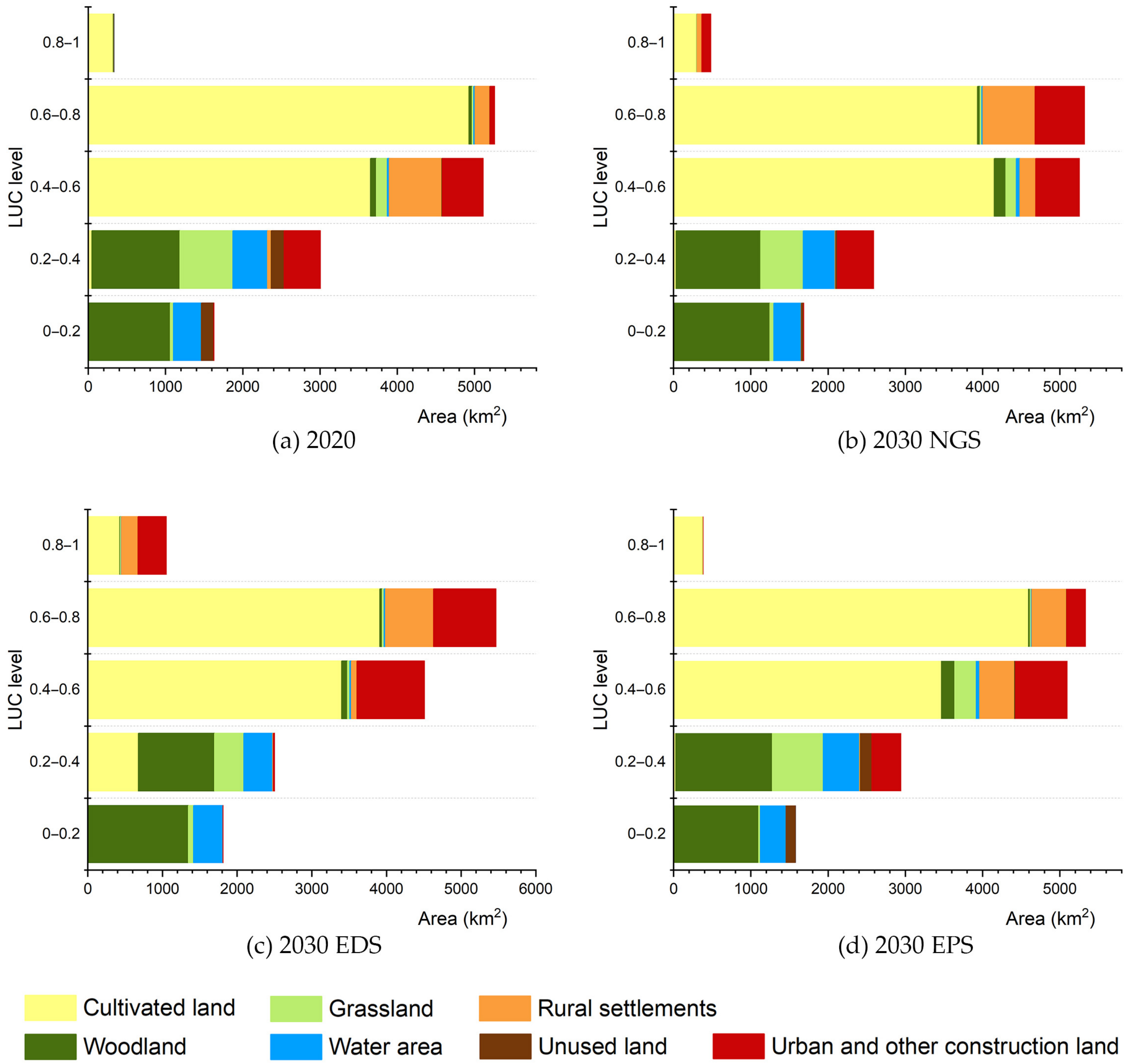

Figure 9. The land use area for each level of land use conflict.

Table 3. Global Moran's I index of LUCs.

Spatial Autocorrelation	2020	2030		
		NGS	EDS	EPS
Moran's I	0.76	0.874	0.884	0.866
z-score	466.102	536.148	541.98	531.312
p-value	0.000	0.000	0.000	0.000

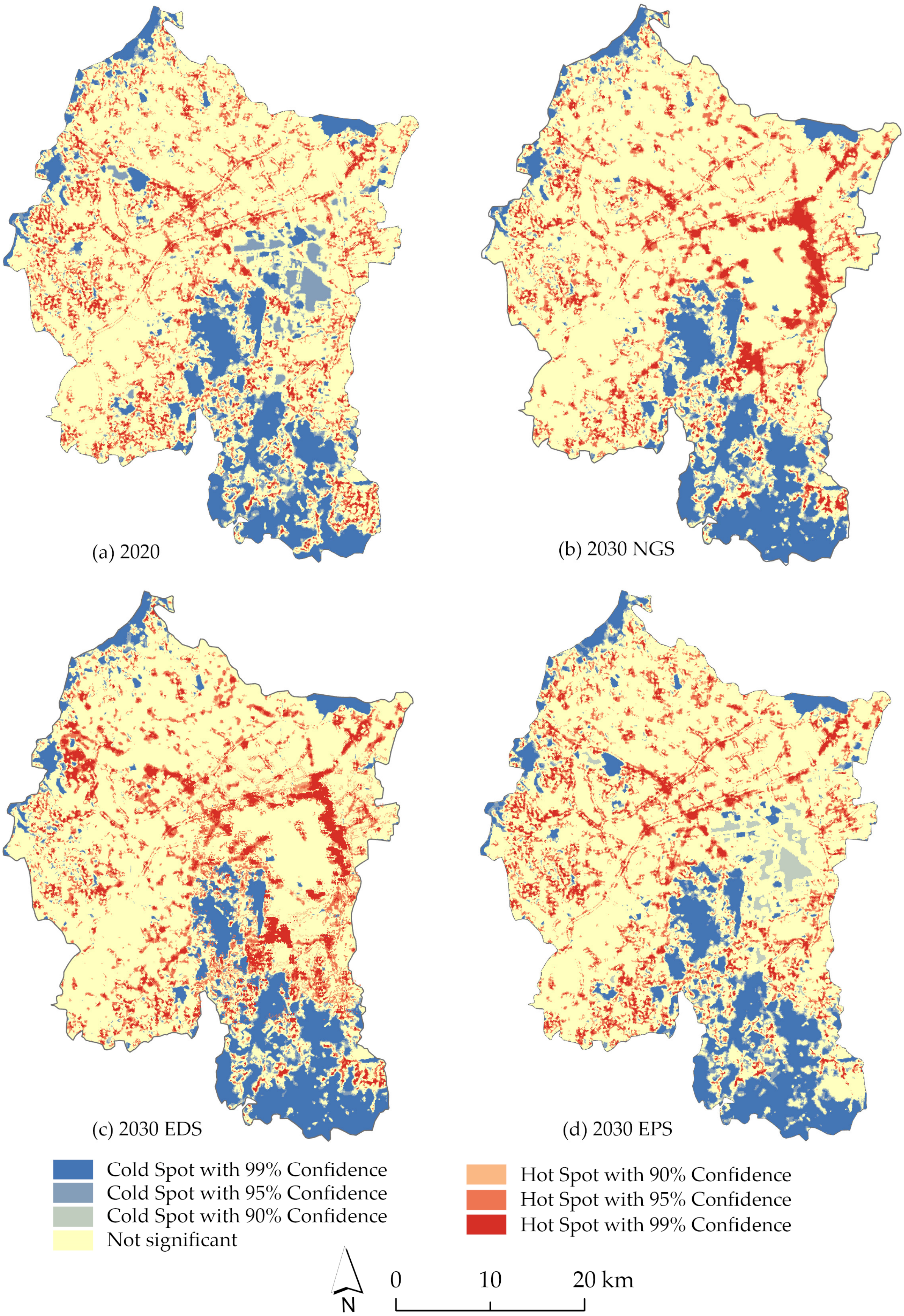

Figure 10. Analysis of local spatial autocorrelation of LUCs.

3.4. Comparison among the Three Scenarios

A statistical analysis of the areas of different land use types (shown in Figure 6) revealed that the areas of cultivated land, woodland, water, and rural settlements were relatively similar across the three scenarios. The grassland, unused land, and urban and other construction land varied considerably in terms of area. In 2020, the area of unused land was 33.86 km^2, and by 2030, all of this had been completely converted under the EDS, only 5.25 km^2 was left under the NGS, and 29.13 km^2 remained under the EPS. The grassland occupied 88.59 km^2 in 2020, and by 2030 it had increased by about 8 km^2 under the EPS, decreased by about 13 km^2 under the NGS, and decreased by about 36 km^2 under the EDS. The area of urban and other construction land increased in all scenarios: 25 km^2 (EPS), 73 km^2 (NGS), and 107.76 km^2 (EDS) respectively. Woodland, grassland, and water are types of ecological lands that can provide ecosystem services, with a total of 406.41 km^2 in 2020 in the study area. They recorded a slight increase of 6.5 km^2 under the NGS, an increase of 30.8 km^2 under EPS, and a decrease of 23.12 km^2 under the EDS. The built-up land, including the rural settlements and urban and other construction land, increased under all scenarios. Its smallest increase was 25 km^2 under the EPS, while its largest increase was under the EDS, which was 4.4 times that under the EPS. Its increase under the NGS was three times that under the EPS. It can also be seen from the comparison of the land use comprehensive dynamics (Table 4) that the overall average index of the EDS was the highest, indicating that land use conversion was most active under this scenario. For each type of land use, the highest value was 8.748, meaning that the conversion of the urban and other construction land under the EDS was the most active. Land use types with relatively high values also included the unused land under the NGS and EDS, the urban and other construction land under the NGS, and the grassland under the EDS, indicating that these land types were also highly converted. Under the EPS, the indices for all land-use types except urban and other construction land, unused land, and woodland were less than one. This suggests that land use change was most stable under this scenario.

Table 4. Land use comprehensive dynamic degree under different scenarios.

Scenarios	Comprehensive Dynamic Degree							
	Overall Average	**Cultivated Land**	**Woodland**	**Grassland**	**Water Area**	**Rural Settlements**	**Unused Land**	**Urban and Other Construction Land**
NGS	1.329	0.598	1.297	1.446	0.300	0.379	8.386	6.864
EDS	1.559	0.603	1.256	3.974	0.425	0.373	6.154	8.748
EPS	0.770	0.569	1.246	0.943	0.002	0.005	1.393	2.359

Further stand deviational ellipse analysis (Figure 11) showed that the expansion direction of built-up land in Liyang in 2030 was "northwest-southeast", which was consistent with 2020. As shown in Table 5, the X-axis distance, Y-axis distance, ellipticity, and ellipse areas all increased, indicating that there was an expansion of built-up land under all of the scenarios. The values of each parameter changed the least under the EPS, indicating that the expansion in built-up land was the lowest under this scenario. In addition, its mean center deviated from 2020 by only 0.31 km, indicating that the built-up land was in a relatively stable state under the EPS. The increase in ellipse area under the EDS was 6%, indicating that the built-up land tended to be dispersed in the expansion direction, and its mean center was shifted 0.93 km to the southwest. The increase in ellipse area under the NGS of 7.9% was the highest among all the scenarios, and the ellipticity of 0.3 was also the highest, indicating that the built-up land was most discrete in the expansion direction, with its center shifting 0.73 km to the south.

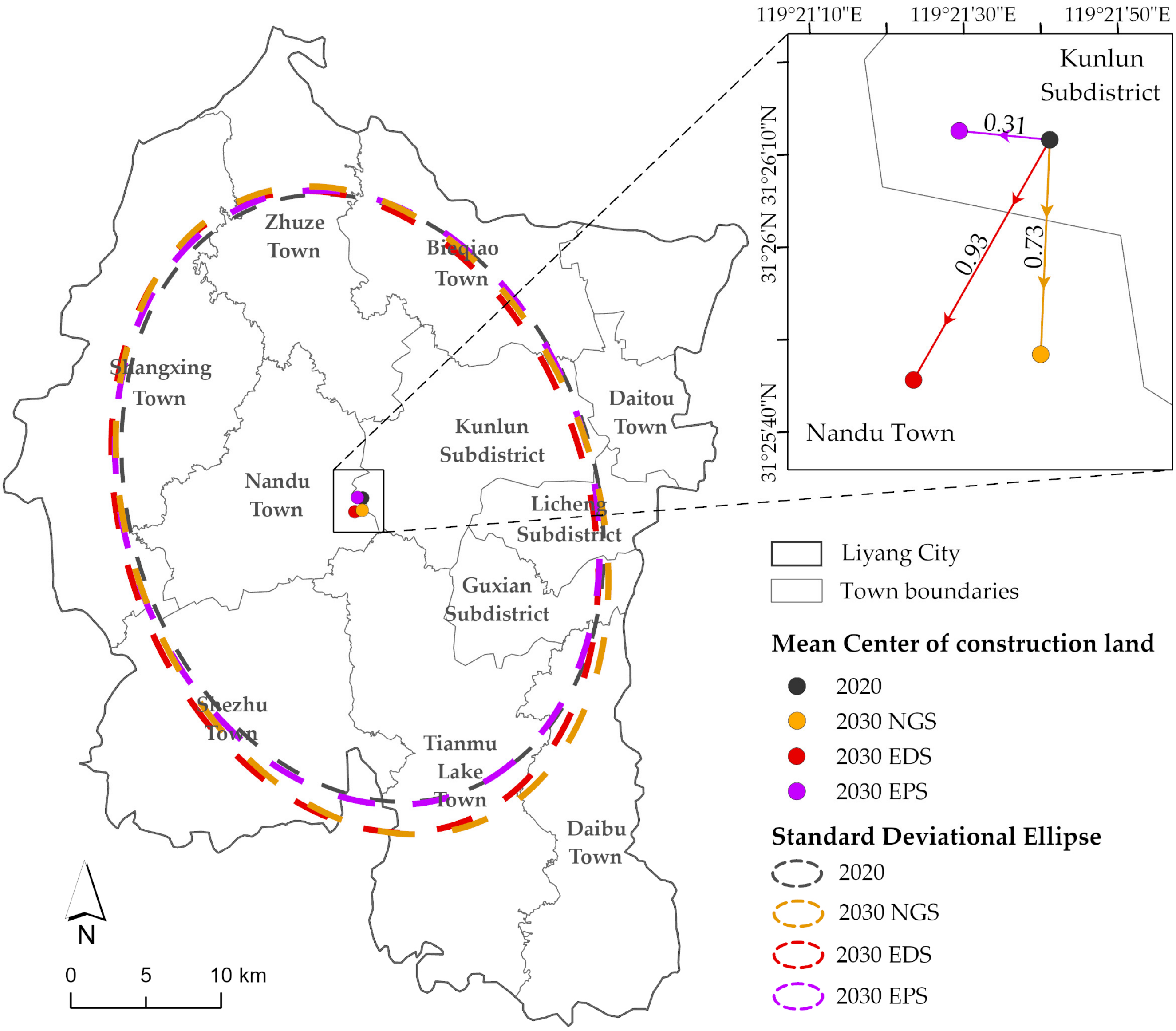

Figure 11. The standard deviational spatial distribution of construction land in 2020 and 2030.

Table 5. Parameter values of standard deviational ellipse.

Year	Scenario	X Distance (km)	Y Distance (km)	Rotation (°)	Ellipticity	Area (km^2)	Central Deviation Distance (km)
2020		13.78	18.36	156.27	0.249	794.85	
2030	NGS	13.85	19.72	155.09	0.300	857.71	0.31
	EDS	13.79	19.45	156.30	0.291	842.41	0.93
	EPS	13.88	18.55	157.00	0.251	808.73	0.73

3.5. Relationship between Land Use Conflicts and Land Use Change

Table 6 shows the quantitative changes in land use conversion from 2020 to 2030 at each level of LUCs under different scenarios. The total areas of land use conversion were 239.36 km^2 under the EDS, 203.98 km^2 under the NGS, and 118.14 km^2 under the EPS. The conversion area in the high and higher levels was 68.21% in the EDS, while this was 46.07% in the NGS and 12.87% in the EPS. As noted in Section 3.2, the average conflict index for the EDS was 0.508, which was higher than the values for the other two scenarios, 0.500 for the NGS and 0.498 for the EPS. This indicates that the degree of land use conversion was closely related to the intensity of land use conflict. Overall, the more land use conversion that occurred in the region, the more intense the land use conflict was.

Table 6. Land use conversion area at each LUC level under different scenarios.

Land-Use Conflict Level		NGS		EDS		EPS	
		LU Conversion Area (km^2)	Ratio (%)	LU Conversion Area (km^2)	Ratio (%)	LU Conversion Area (km^2)	Ratio (%)
L1	Lower	30.61	15.01	32.48	13.57	16.42	13.90
L2	Low	37.07	18.17	18.01	7.52	43.68	36.97
L3	Moderate	42.33	20.75	25.60	10.70	42.84	36.26
L4	High	73.63	36.10	100.27	41.89	15.08	12.77
L5	Higher	20.34	9.97	63.00	26.32	0.12	0.10
SUM		203.98	100	239.36	100	118.14	100

Figure 12 displays the area of each land use type that was converted at each level of land use conflict (LUC) under different scenarios. In all scenarios, a considerable portion of the converted area was attributed to the built-up land, woodland, and cultivated land, while grasslands and unused land came next in terms of their contribution. The proportion of converted cultivated land was most stable under the EPS, remaining between 30% and 50% for all LUC levels, while it was more variable under the other two scenarios, ranging from less than 10% to more than 40%. Under the EPS, the proportion of converted woodland was the highest at 43.2%; this was much higher than that under the other two scenarios, namely, 26.3% under the NGS and 22.61% under the EDS. From L1 to L5 of the land use conflict, the converted area of woodland decreased, and this was mainly concentrated in L1 and L2. The converted area for the urban and other construction land showed the opposite trend. From L1 to L5, the proportion of converted area for the urban and other construction land under the EPS increased from 0.2% to 47.6% at L4 and then decreased to 13.35% at L5. Under the NGS, it increased from 6.9% at L1 to 47% at L3 and then remained stable. Under the EDS, it increased from 1.68% at L1 to 49% at L5. This suggests that the intensity of conversion for urban and other construction land was closely related to the level of land use conflict. The most typical area, in this case, was the urban-rural interface area around the city center, which recorded the highest level of land use conflicts (Figure 8) and significant hotspots (Figure 10). This was because this area was the main region for future construction and expansion (Figure 5), and frequent and intense land use changes often generate severe land use conflicts. Even though the area of other land use types that was converted was relatively small, there was still some relationship between the amount of land use conversion and the level of conflict over land use. The land use dynamic degree is a measure of the intensity of change in land use. The Pearson correlation between the dynamic values for each land use type and the average land use conflict index is shown in Figure 13. Overall, there was a positive correlation between the land use dynamic degree and the average land use conflict, with a correlation coefficient of 0.84 recorded. For each land use type, there was also a positive correlation between land use dynamism and conflict, with the exception of the woodland.

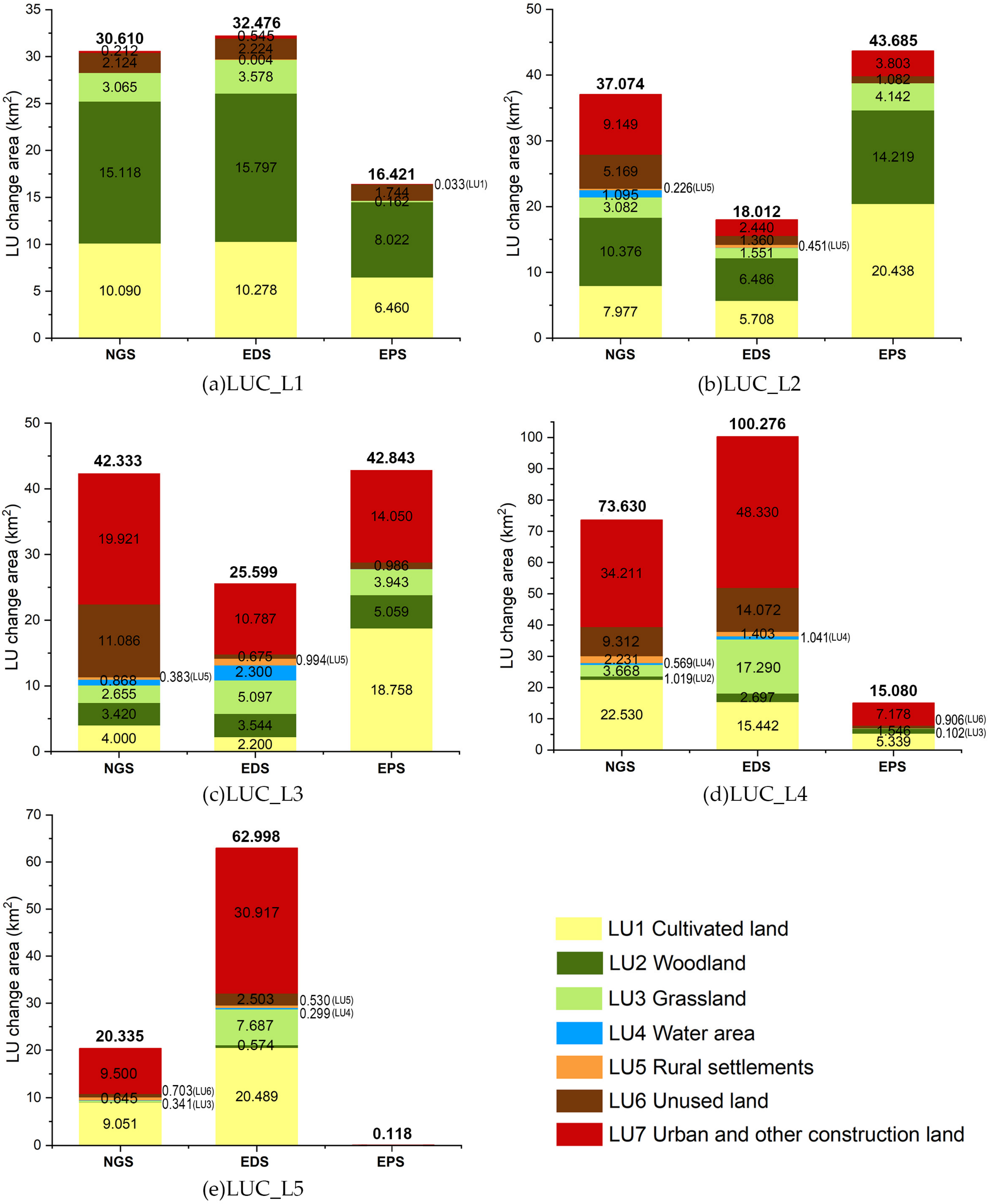

Figure 12. Land use transition area at each LUC level under different scenarios.

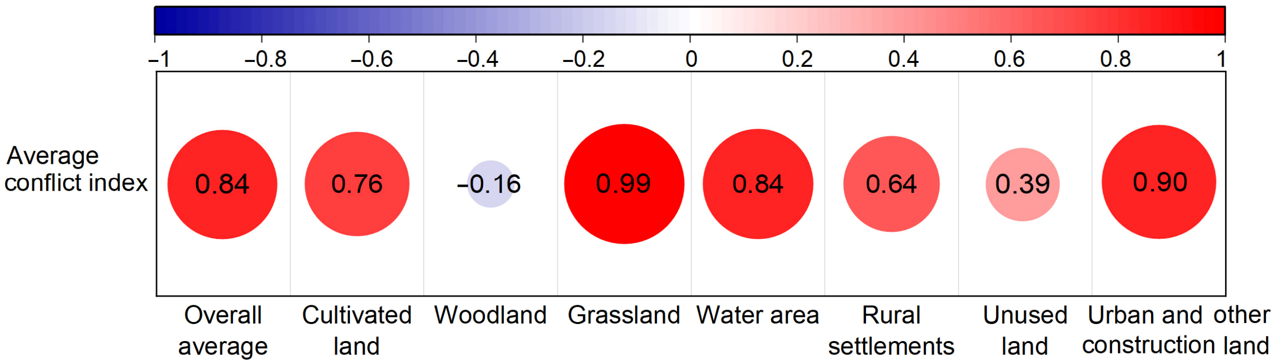

Figure 13. Pearson correlation coefficients between average conflict index and land use comprehensive dynamic degrees.

4. Discussion

4.1. Practical Implications for Land Use

The three simulation scenarios represented different development needs. The NGS continued the trend of previous years without external intervention. The EDS focused on economic profit, with an emphasis on industrial development and urbanization. The EPS focused on ecological conservation, with the setting of restricted areas. Both NGS and EDS were characterized by an increase in land use conflicts. Considering that Liyang has all-for-one tourism as one of its long-term development goals, the EPS may be the most suitable choice in the future, as it can better maintain good natural resources and the ecological environment. Multi-simulation of future land use can only provide some reference value for policy-making; scientific strategies should also be developed from a practical perspective and tailored to local conditions. The matters that need attention include the following:

(1) In addition to protecting Liyang's ecological sources as restricted areas, ecological restoration should also be carried out in conjunction with the distribution of ecological corridors and nodes, and ecological monitoring should be conducted in a timely manner to ensure the ecological security pattern of Liyang is well preserved. During the development and operation of tourism projects, tourist capacity should be reasonably controlled, and an environmental impact assessment of tourism behavior should be carried out, so as to achieve the coordinated development of ecological protection and tourism in the city.

(2) The cultivated land, which accounts for more than 50% of the city, is a key area for regulating land use conflicts between urban and rural areas. In this study, under all scenarios, the area of the converted cultivated land was more than 50 km^2. It is inevitable that urban sprawl will occupy a large amount of arable land. The resulting year-on-year decline in grain production will put enormous pressure on maintaining food security in the region. Therefore, it is necessary to strictly define a red line for basic farmland protection, improve the level of agricultural mechanization, actively promote smart agriculture, and improve the quality of existing farmland in Liyang.

(3) As shown in the previous analyses, there was a significant positive correlation between the dynamism of built-up land and the intensity of land use conflict. Regions with high levels of conflict tended to have large amounts of built-up land being converted. This was most typical for areas around the city center, where urban expansion led to serious land use conflicts. As a result, it is important to strictly control the urban growth boundary and establish an ecological buffer zone to prevent uncontrolled urban expansion. In addition, the expansion direction of the built-up land was found to be northwest-southeast. The Caoshan Development Zone in the northwest, Tianmu Lake, and Nanshan Bamboo Sea in the south are the driving force of built-up land expansion, and construction in these areas needs to be carefully managed to avoid serious land use conflicts.

4.2. Methodological Advantages

The research idea of this paper is to carry out a dynamic analysis of current and future land use conflicts, based on land changes from the past to the present and multi-scenario simulations of future land use. As an empirical study, this paper complements the lack of consideration of the future development trend of LUCs in the current research. It also provides forward-looking strategies for territorial spatial planning that are in line with China's national conditions of scarce land resources and a pronounced contradiction between people and land under rapid development.

This paper further explored the relationship between the intensity of land use changes and land use conflicts by analyzing their characteristics. While previous studies have mostly analyzed the relationship qualitatively, this study used Pearson's correlation analysis to show quantitatively and precisely that the more land use talked about, the more intense the land use conflict.

From the perspective of dynamic land use conflict, the areas to focus on in Liyang are suggested so that city leaders can better formulate policies and strategies when carrying out land development. This case can also provide a reference and ideas for territorial spatial planning at the county level.

4.3. Limitations and Future Directions

In terms of selecting drivers of land use change, this paper draws on previous studies and selects variables that can be spatially quantified, covering geographic, meteorological, soil, location, and socio-economic factors. However, land use change is also influenced by many factors that are difficult to collect and quantify, such as politics, land rights, and cultural practices. Future research should consider how these factors can be incorporated into land use simulation models.

The configuration of the parameters of land use simulation has a direct impact on the simulation results. In this study, although the accuracy verification met the required threshold, there is still potential room for further refinement. For example, various policy factors were not taken into account in the parameter settings. Further, the land use simulation under the EPS defined only ecological land as restricted areas, ignoring the fact that cultivated land can also provide a habitat for wildlife. In addition, the simulation was based solely on the CLUMondo model, and future multi-platform verification in conjunction with other models is required to improve the accuracy of the land use simulation.

This study measures land use conflict from a landscape ecology perspective by evaluating a region's complexity, fragility, and stability. However, land use conflict is a multifaceted concept that encompasses not only ecological considerations but also social, institutional, cultural, land tenure, and structure-function conflicts [71]. The mechanisms and manifestations of land use conflicts are highly complex, and some conflicts cannot be spatially represented. Therefore, it is necessary to develop a comprehensive, multi-indicator evaluation system that combines qualitative and quantitative evaluations from different perspectives to measure land use conflict objectively and comprehensively.

5. Conclusions

Due to the acceleration of urbanization, human demand for land resources has continued to grow. Coupled with the growing problems of global climate change, population growth, and environmental pollution, the globe's limited land resources are under great pressure. Land use conflicts reflect the mismatch and imbalance between land use allocation and societal development needs. By predicting and analyzing regional land use conflicts, the contradictory relationship between future urban development and land resources can be identified, the intensification of conflicts can be prevented in a timely manner, and the rational use of land resources can be realized. Liyang, a county-level city in China which has adopted the all-for-one tourism approach as its development engine, is facing conflicting trade-offs between economic, environmental, and social benefits in the process of urbanization. Presenting Liyang as a research case, this paper used the CLUMondo model to simulate land use in 2030 under three scenarios, namely, the NGS, EDS, and EPS, based on the land use map of 2020. Then, the land use conflicts under the different scenarios were measured by calculating the complexity, vulnerability, and stability of the region. Finally, by comparing and analyzing the characteristics of land use conversion and land use conflict, and discussing the relationship between the two, strategies and key areas for future land use planning were provided. The findings of the study were as follows:

(1) Under the three scenarios, there were only slight changes to the water area and rural settlements, while the cultivated land experienced a significant decrease, and the urban and other construction land showed a remarkable increase. Regarding their total amount of land conversion and total dynamic degree of land use, the scenarios were ranked as follows: EDS > NGS > EPS. The largest converted areas among all land use types were cultivated land, woodland, unused land, and urban and construction land. The higher land use dynamic degree included the urban and other construction land under all the scenarios, the unused land under the NGS and EDS, and the grassland under the EDS.

(2) All of the average land use conflict indices under the three scenarios were higher than the 2020 value, with the highest recorded under the EDS and the lowest under the EPS. The spatial distribution of LUCs showed little change under the EPS, but significant intensity under the NGS and EDS. Under the NGS, the most obvious high-level land use conflict occurred around the city center area. Under the EDS, besides the city center's surroundings, the most obvious high-level conflict areas also included the area around the Caoshan Development Zone in the northwest and the Nanshan Bamboo Sea in the south.

(3) The land use conflicts were found to be closely related to the land use change. In general, the more intensive the land conversions, the higher the land use conflicts. The Pearson correlation analysis showed that the average land use conflict index in the study area was significantly positively correlated with the overall average land use comprehensive dynamic degree. For each land use type, the correlation between the land use dynamics and the average land use conflict index was positive, except for the woodland.

(4) The EPS was found to be the most suitable for the development of all-for-one tourism in Liyang, as it recorded the least land use conflicts among the three scenarios. In the future, particular attention should be paid to the areas around the city center, Caoshan Development Zone, and the Nanshan Bamboo Sea, where high-intensity land use conflicts are likely to occur. It is also necessary to protect and restore the key areas of ecological security patterns and to ensure the quantity and quality of arable land in order to maintain food security in the city.

Supplementary Materials: The following supporting information can be downloaded at: https://www.mdpi.com/article/10.3390/land12040917/s1, Table S1: Policy reference for scenario setting; Table S2: Correlation matrix of driving factors; Figure S1: Driving factors of land use change; Table S3: Regression analysis; Table S4: Change rate of demand for land use services under different scenarios; Figure S2: Spatial restrictions for land use simulation; Table S5: Conversion resistance of land use types under different scenarios; Table S6: Conversion matrix under different scenarios; Table S7: Kappa coefficients of simulation validation.

Author Contributions: Conceptualization, X.F. and Y.C.; methodology, validation, data curation, writing—original draft preparation, X.F.; project administration, Y.C.; software, X.F.; writing—review and editing, supervision, X.F. and Y.L. All authors have read and agreed to the published version of the manuscript.

Funding: This research was funded by China Postdoctoral Science Foundation, grant number 2020M671306.

Data Availability Statement: The data presented in this study are available on request from the corresponding author.

Acknowledgments: We would like to express our gratitude to National Tibetan Plateau Data Center (http://data.tpdc.ac.cn) (accessed on 12 January 2023) for providing the soil data. We also thank the reviewers for providing constructive comments on this manuscript.

Conflicts of Interest: The authors declare no conflict of interest.

References

1. Zuo, Q.; Zhou, Y.; Wang, L.; Li, Q.; Liu, J. Impacts of future land use changes on land use conflicts based on multiple scenarios in the central mountain region, China. *Ecol. Indic.* **2022**, *137*, 108743. [CrossRef]
2. Fan, S.; Cheng, C.; Liu, Y.; Zhang, H.; Yu, R. Review and prospect on land use/cover research in China. *Areal Res. Dev.* **2017**, *36*, 94–101.
3. Wang, Y.; Dai, Y.; Jia, C.; Tan, Y.; Sun, M.; Li, H. Spatiotemporal change analysis of land use/cover in Xuzhou from 2010 to 2020. *Terr. Nat. Rec. Study* **2023**, *1*, 35–39.
4. Steo, K.C.; Guneralp, B.; Hutyra, L.R. Global forecasts of urban expansion to 2030 and direct impacts on biodiversity and carbon pools. *Proc. Natl. Acad. Sci. USA* **2012**, *109*, 16083–16088. [CrossRef] [PubMed]
5. Bai, E.; Xue, B. A review of influences of land use and land cover change on ecosystems. *Chin. J. Plant Ecol.* **2022**, *44*, 543–552.
6. United Nations. Agenda 21. Available online: https://sdgs.un.org/publications/agenda21 (accessed on 17 March 2023).
7. Turner, B.L.; Skole, D.; Sanderson, S.; Fischer, G.; Fresco, L.; Leemans, R. Land use and land-cover change: Science/research plan. In Proceedings of the International Geosphere-Biosphere Program Secretariat, Stockholm, Sweden, 1 January 1995.
8. Ojima, D.; Moran, E.; McConnell, W.; Smith, M.S.; Laumann, G.; Morais, J.; Young, B. *Global Land Project: Science Plan and Implementation Strategy*; IGBP Report No. 53/IHDP Report No. 19; IGBP Secretariat: Stockholm, Sweden, 2005.
9. Global LAND Programme. Available online: https://glp.earth/ (accessed on 17 March 2023).
10. Turner, B.L.; Lambin, E.F.; Reeberg, A. Land Change Science Special Feature: The emergence of land change science for global environmental change and sustainability. *Proc. Natl. Acad. Sci. USA* **2007**, *104*, 20666–20671. [CrossRef]
11. Lambin, E.F.; Turner, B.L.; Geist, H.J.; Agbola, S.B.; Angelsen, A.; Bruce, J.W.; Coomes, O.T.; Dirzo, R.; Fischer, G.; Folke, C.; et al. The causes of land-use and land-cover change: Moving beyond the myths. *Glob. Environ. Chang.* **2001**, *11*, 261–269. [CrossRef]
12. Wolff, S.; Schrammeijer, E.A.; Schulp, C.J.E.; Verburg, P.H. Meeting Global Land Restoration and Protection Targets: What Would the World Look Like in 2050. *Glob. Environ. Chang.* **2018**, *52*, 259–272. [CrossRef]
13. Xie, Y.; Gao, P.; Ye, S.; Shen, S.; Zhang, X. Review and prospect of land change simulation model CLUMondo. *Geomat. World* **2022**, *29*, 7–12.
14. Qiao, Z.; Jiang, Y.; He, T.; Lu, Y.; Xu, X.; Yang, J. Land use change simulation: Progress, challenges, and prospects. *Acta Ecol. Sin.* **2022**, *42*, 5165–5176.
15. Ren, Y.; Lu, Y.; Comber, A.; Fu, B.; Harris, P.; Wu, L. Spatially explicit simulation of land use/land cover changes: Current coverage and future prospects. *Earth-Sci. Rev.* **2019**, *190*, 398–415. [CrossRef]
16. Nie, X.; Lu, B.; Chen, Z.; Yang, Y.; Chen, S.; Chen, Z.; Wang, H. Increase or decrease? Integrating the CLUMondo and InVEST models to assess the impact of the implementation of the Major Function Oriented Zone planning on carbon storage. *Ecol. Indic.* **2020**, *118*, 106708. [CrossRef]
17. Chang, Y. The Simulation and Trend Prediction of Sandy Land Change in Alxa Area Based on CLUMondo Model. Master's Thesis, Lanzhou Jiaotong University, Lanzhou, China, 20 April 2021.
18. Liu, X.; Zhang, Z.; Li, M.; Fu, Y.; Hui, Y. Spatial conflict simulation of land-use based on human-land-landscape elements intercoordination: A case study in Tianjin, China. *Environ. Monit. Assess.* **2022**, *194*, 317. [CrossRef]
19. Hui, E.C.M.; Bao, H. The logic behind conflicts in land acquisitions in contemporary China: A framework based upon game theory. *Land Use Policy* **2013**, *30*, 373–380. [CrossRef]
20. Zhang, J.; Chen, Y.; Zhu, C.; Huang, B.; Gan, M. Identification of Potential Land-Use Conflicts between Agricultural and Ecological Space in an Ecologically Fragile Area of Southeastern China. *Land* **2021**, *10*, 1011. [CrossRef]
21. Kim, I.; Arnhold, S. Mapping environmental land use conflict potentials and ecosystem services in agricultural watersheds. *Sci. Total Environ.* **2018**, *630*, 827–838. [CrossRef]
22. Kang, Z.; Wang, S.; Xu, L.; Yang, F.; Zhang, S. Suitability assessment of urban land use in Dalian, China using PNN and GIS. *Nat. Hazards* **2021**, *106*, 913–936. [CrossRef]
23. Ioja, C.; Nita, M.; Vanau, G.O.; Onose, D.A.; Garvilidis, A.A. Using multi-criteria analysis for the identification of spatial land-use conflicts in the Bucharest Metropolitan Area. *Ecol. Indic.* **2014**, *42*, 112–121. [CrossRef]
24. Brown, G.; Raymond, C.M. Methods for identifying land use conflict potential using participatory mapping. *Landsc. Urban Plan.* **2014**, *122*, 196–208. [CrossRef]
25. Zhang, H.; Zeng, Y.; Jin, X.; Shu, B.; Zhou, Y.; Yang, X. Simulating multi-objective land use optimization allocation using multi-agent system—A case study in Changsha, China. *Ecol. Modell.* **2016**, *320*, 334–337. [CrossRef]
26. Chen, Y.; Xie, B.; Zhong, D.; Wu, L.; Zhang, A. Predictive simulation of ecological space based on a particle swarm optimization-Markov composite model: A case study for Chang-Zhu-Tan urban agglomerations. *Acta Ecol. Sin.* **2018**, *38*, 55–64.
27. Wang, T.; Cao, J.; Zhao, Y.; Han, L.; Liu, Z. Evaluation of land ecosystem health in Shaanxi Province, Northwest China based on PSR model. *Chin. J. Appl. Ecol.* **2021**, *32*, 1563–1572.
28. Meng, B. Analysis and Optimization Strategy Territorial of Space Function in Yibin. Ph.D. Thesis, University of Chinese Academy of Sciences, Beijing, China, September 2020.
29. Li, C.; Wu, J. Land use transformation and eco-environmental effects based on production-living-ecological spatial synergy: Evidence from Shaanxi Province, China. *Environ. Sci. Pollut. Res.* **2022**, *29*, 41492–41504. [CrossRef] [PubMed]
30. Omrani, H.; Parmentier, B.; Helbich, M.; Pijanowski, B. The land transformation model-cluster framework: Applying k-means and the Spark computing environment for large scale land change analytics. *Environ. Model. Softw.* **2019**, *111*, 182–191. [CrossRef]

31. Domingo, D.; Palka, G.; Hersperger, A.M. Effect of zoning plans on urban land-use change: A multi-scenario simulation for supporting sustainable urban growth. *Sustain. Cities Soc.* **2021**, *69*, 102833. [CrossRef]
32. Bacau, S.; Domingo, D.; Palka, G.; Pellissier, L.; Kienast, F. Integrating strategic planning intentions into land-change simulations: Designing and assessing scenarios for Bucharest. *Sustain. Cities Soc.* **2021**, *76*, 103446. [CrossRef]
33. Aburas, M.M.; Ho, Y.M.; Ramli, M.F.; Ash'aari, Z.H. The simulation and prediction of spatio-temporal urban growth trends using cellular automata models: A review. *Int. J. Appl. Earth Obs.* **2016**, *52*, 380–389. [CrossRef]
34. Arunyawat, S.; Shrestha, R.P. Simulating future land use and ecosystem services in Northern Thailand. *J. Land Use Sci.* **2018**, *13*, 145–165. [CrossRef]
35. Jin, G.; Deng, X.; Chu, X.; Wang, Y. Optimization of land-use management for ecosystem service improvement: A review. *Phys. Chem. Earth* **2017**, *101*, 70–77. [CrossRef]
36. Steinhausser, R.; Siebert, R.; Steinfuhrer, A.; Hellmich, M. National and regional land-use conflicts in Germany from the perspective of stakeholders. *Land Use Policy* **2016**, *49*, 183–194. [CrossRef]
37. Xie, Z.; Ma, Z.; Liu, J. Conflicts in Land Use in Marine Protected Areas: The Case of the Yellow River Delta, China. *J. Coastal Res.* **2014**, *30*, 1307–1314. [CrossRef]
38. Song, J.; Meng, J.; Zhu, L.; Cheng, H. Spatial-temporal pattern of land use conflict in China and its multilevel driving mechanisms. *Sci. Total Environ.* **2021**, *801*, 149697.
39. Torre, A.; Melot, R.; Magsi, H.; Bossuet, L.; Cadoret, A.; Caron, A.; Darly, S.; Jeanneaux, P.; Kirat, T.; Pham, H.V.; et al. Identifying and measuring land-use and proximity conflicts: Methods and identification. *SpringerPlus* **2014**, *3*, 85. [CrossRef] [PubMed]
40. Cui, J.; Kong, X.; Chen, J.; Sun, J.; Zhu, Y. Spatially Explicit Evaluation and Driving Factor Identification of Land Use Conflict in Yangtze River Economic Belt. *Land* **2021**, *10*, 43. [CrossRef]
41. Yu, L.; Cai, Y. Research on spatial regulation of land use planning and coordinated development of regional economy: An analytical framework. *J. Nat. Resour.* **2017**, *32*, 1445–1456.
42. Zou, L.; Liu, Y.; Wang, Y. Research progress and prospect of land-use conflicts in China. *Prog. Geogr.* **2020**, *39*, 298–309. [CrossRef]
43. Pontius, R.G.; Huang, J.; Jiang, W.; Khallaghi, S.; Lin, Y.; Liu, J.; Quan, B.; Ye, S. Rules to Write Mathematics to Clarify Metrics Such as the Land Use Dynamic Degrees. *Landsc. Ecol.* **2017**, *32*, 2249–2260. [CrossRef]
44. Yang, K.; Wang, X.; Zhao, P.; Liu, X.; Zhang, Y. The Study of Driving Forces of Land Use Transformation in the Pearl River Delta during 1990 to 2010. In Proceedings of the 2nd International Workshop on Renewable Energy and Development, Guilin, China, 20 April 2018.
45. Li, P.; Zuo, D.; Xu, Z.; Zhang, R.; Han, Y.; Sun, W.; Sun, W.; Pang, B.; Ban, C.; Kan, G.; et al. Dynamic changes of land use/cover and landscape pattern in a typical alpine river basin of the Qinghai-Tibet Plateau, China. *Land Degrad. Dev.* **2021**, *32*, 4327–4339. [CrossRef]
46. Meng, J.; Jiang, S.; Laba, Z.; Zhang, W. The Spatial and Temporal Analysis of Land Use Conflict in the Middle Reaches of the Heihe River Based on Landscape Pattern. *Chin. Geogr. Sci.* **2020**, *40*, 1553–1562.
47. Qiu, G.; Wang, Y.; Guo, S.; Niu, Q.; Qin, L.; Zhu, D.; Gong, Y. Assessment and Spatial-Temporal Evolution Analysis of Land Use Conflict within Urban Spatial Zoning: Case of the Su-Xi-Chang Region. *Sustainability* **2022**, *14*, 2286. [CrossRef]
48. Xiao, P.; Xu, J.; Zhao, C. Conflict Identification and Zoning Optimization of "Production-Living-Ecological" Space. *Int. J. Environ. Res. Public Health* **2022**, *19*, 7990. [CrossRef] [PubMed]
49. Chen, S.; Ai, D.; Fu, Y. Spatial conflict measurement and influencing factors based on ecological security. *J. China Agric. Univ.* **2020**, *25*, 141–150.
50. Chen, Z.; Feng, X.; Hong, Z.; Li, Y. Calculation and analysis of spatial conflicts in land use of Nanchang city. *Areal Res. Dev.* **2020**, *39*, 150–155.
51. Zhao, X.; Tang, F.; Zhang, P.; Hu, B.; Xu, L. Dynamic simulation and characteristic analysis of county production-living ecological spatial conflicts based on CLUE-S mode. *Acta Ecol. Sin.* **2019**, *39*, 5879–5908.
52. Verburg, P. The CLUMondo Land Use Change Model: Manual and Exercises. Institute for Environmental Studies, Amsterdam, Netherlands. December 2015. Available online: https://www.environmentalgeography.nl/site/ (accessed on 17 March 2023).
53. Yin, L.; Dai, E.; Xie, G.; Zhang, B. Effects of Land-Use Intensity and Land Management Policies on Evolution of Regional Land System: A Case Study in the Hengduan Mountain Region. *Land* **2021**, *10*, 5. [CrossRef]
54. Rahman, M.T.U.; Tabassum, F.; Rasheduzzaman, M.; Saba, H.; Sarkar, L.; Ferdous, J.; Uddin, S.Z.; Islam, A.Z.M.Z. Temporal dynamics of land use/land cover change and its prediction using CA-ANN model for southwestern coastal Bangladesh. *Environ. Monit. Assess.* **2017**, *189*, 11. [CrossRef]
55. Guo, R.; Lu, B.; Chen, K. Dynamic simulation of multi-scenario land use change based on CLU-Mondo model: A case study of coastal cities in Guangxi. *Remot. Sens. Land Resour.* **2020**, *32*, 176–183.
56. Liyang Introduces the "14th Five-Year" Territorial Tourism Development Plan. Available online: http://www.liyang.gov.cn/index.php?c=phone&a=show&id=168037&catid=40409 (accessed on 4 April 2023).
57. Notice of Liyang Government Office on Printing and Issuing the "Special Planning Work Plan for Liyang Master Plan (2016–2030)". Available online: http://www.liyang.gov.cn/html/czly/2018/OPEHQFEM_0216/5690.html (accessed on 4 April 2023).
58. Liyang Territorial Spatial Master Plan (2021–2035) (Draft) Public Notice. Available online: http://www.liyang.gov.cn//html/czly/2022/NDKMAMKM_1221/30553.html (accessed on 4 April 2023).

59. Wang, C.; Yu, C.; Chen, T.; Feng, Z.; Hu, Y.; Wu, K. Can the establishment of ecological security patterns improve ecological protection? An example of Nanchang, China. *Sci. Total Environ.* **2020**, *740*, 140051. [CrossRef]
60. Zhu, W.; Gao, Y.; Zhang, H.; Liu, L. Optimization of the land use pattern in Horqin Sandy Land by using the CLUMondo model and Bayesian belief network. *Sci. Total Environ.* **2020**, *739*, 139929. [CrossRef]
61. Van Asselen, S.; Verburg, P.H. Land cover change or land-use intensification: Simulating land system change with a global-scale land change model. *Glob. Chang. Biol.* **2013**, *32*, 2249–2260. [CrossRef]
62. Ornetsmuller, C.; Verburg, P.H.; Heinimann, A. Scenarios of land system change in the Lao PDR: Transitions in response to alternative demands on goods and services provided by the land. *Appl. Geogr.* **2016**, *75*, 1–11. [CrossRef]
63. Malek, Z.; Verburg, P.H.; Geijzendorffer, I.R.; Bondeau, A.; Cramer, W. Global change effects on land management in the Mediterranean region. *Global Environ. Chang.* **2018**, *50*, 238–254. [CrossRef]
64. Chen, C.I.; Huang, S.J. The necessary and sufficient condition for GM (1,1) grey prediction model. *Appl. Math. Comput.* **2013**, *219*, 6152–6162. [CrossRef]
65. Fan, X.; Cheng, Y.; Tan, F.; Zhao, T. Construction and Optimization of the Ecological Security Pattern in Liyang, China. *Land* **2022**, *11*, 1641. [CrossRef]
66. Monserud, R.A.; Leemans, R. Comparing global vegetation maps with the Kappa-statistic. *Ecol. Model.* **1992**, *62*, 275–293. [CrossRef]
67. Liu, M.; Hu, Y.; Chang, Y.; He, H.; Bu, R. Analysis of temporal predicting abilities for the CLUE-S land use model. *Acta Ecol. Sin.* **2009**, *29*, 6110–6119.
68. Li, W.; Zhu, C.; Wang, H.; Xu, B. Multi-scale spatial autocorrelation analysis of cultivated land quality in Zhejiang province. Trans. Chin. *Soc. Agric. Eng.* **2016**, *32*, 239–245.
69. Cressie, N.; Kang, E.L. Hot enough for you? A spatial exploratory and inferential analysis of North American climate-change projections. *Math. Geosci.* **2016**, *48*, 107–121. [CrossRef]
70. Liu, Y.; Li, Y.; Yi, X.; Cheng, X. Spatial evolution of land use intensity and landscape pattern response of the typical basins in Guizhou Province, China. *Ying Yong Sheng Tai Xue Bao J. Appl. Ecol.* **2017**, *28*, 3691–3702.
71. Zhou, D.; Lin, Z.; Lim, S.H. Spatial characteristics and risk factor identification for land use spatial conflicts in a rapid urbanization region in China. *Environ. Monit. Assess.* **2019**, *191*, 677. [CrossRef]